Republic of Iraq
Ministry of Higher Education & Scientific Research
University of Babylon
College of Education for Pure Sciences
Department of Physics

Effect of Thickness on Electrical and Optical Properties for (PMMA-PbO) Nanocomposites and their Applications

A Thesis
Submitted to the Council of the College of Education for Pure Sciences, University of Babylon in Partial Fulfillment of the Requirements for the Degree of Master in Education / Physics

By

Bashaer Aid Kazim Matroud

B. Sc. in Physics
(University of Karbala- 2019)

Supervised by

Prof. Dr. Sameer H. Hadi Al- Nesrawy

2022 A.D. **1444A.H.**

بِسْمِ ٱللَّهِ ٱلرَّحْمَٰنِ ٱلرَّحِيمِ

أَمَّنْ هُوَ قَٰنِتٌ ءَانَآءَ ٱلَّيْلِ سَاجِدًا وَقَآئِمًا يَحْذَرُ ٱلْءَاخِرَةَ وَيَرْجُواْ رَحْمَةَ رَبِّهِۦ ۗ قُلْ هَلْ يَسْتَوِى ٱلَّذِينَ يَعْلَمُونَ وَٱلَّذِينَ لَا يَعْلَمُونَ ۗ إِنَّمَا يَتَذَكَّرُ أُوْلُواْ ٱلْأَلْبَٰبِ ﴿٩﴾

صَدَقَ اللهُ العَظِيمُ

سورة الزمر

الآية (9)

Dedications

To Mesopotamia (Iraq) with honor and dignity…

To those who lost their lives in a war without committing any crime
To my first and dearest teacher, my father
To my mother, whose love is planted in my heart
To my brothers and sisters,
To my close friends,
To my teachers
who provided me with the keys to success

Allah bless you all

Bashaer Aid

Acknowledgments

Praise be to ALLAH, His majesty for his uncountable blessings, and best prayers and peace be unto his best Messenger Mohammed, his pure descendants, and his noble companions.

I wish to express my deepest gratitude and appreciation to my supervisor Prof. Dr. Sameer H.AL-Nesrawy for suggesting this project, guidance, support, and encouragement through the research work.

Thanks to the Deanship of the College of Education for Pure Sciences-University of Babylon and the Department of Physics for offering me the opportunity to complete my research. I also would like to express my gratitude thanks to all teachers, instructors and students of Department of Physics for their assistance and supports.

Eventually, many thanks who always support me and alleviate difficulties I have faced during my work and everyone who helped me in a way or another during my preparation of this thesis ,special thanks to the professors of the Advanced Physics Laboratory. I apologize for who I miss mentioned. I wish success to all.

Bashaer Aid

Summary

This study found on the effect of the film thickness on the optical and electrical properties of (PMMA-PbO) nanocomposites. (PMMA-PbO) nanocomposites were prepared by casting method, with an average particle size 66 nm and weight percentages of lead oxide nanoparticles (0,1,2, and 3) wt%, micrometer was used to determine the thickness of the samples, and found to be within (60, 120, 220) μm.

The optical microscope images showed that lead oxide nanoparticles form a continuous network inside the polymer at 3wt.%. The FTIR displacement spectra appear in some ranges and change in intensity, and this indicates the absence of a chemical reaction, but rather the occurrence of physical interconnection. The surface morphology of the (PMMA-PbO) nanocomposite films is revealed by using scanning electron microscopy (SEM), which reveals several aggregates randomly distributed on the top surface, which are homogeneous and coherent.

The optical properties show that the absorbance, absorption coefficient, extinction coefficient, refractive index, and dielectric constant (real, imaginary) increased with the increasing film thickness, and concentrations of (PbO) nanoparticles. The energy gap decreased with the increasing of film thicknesses and the concentration of the lead oxide nanoparticles.

The dielectric constant, dielectric loss, and A.C electrical conductivity for (PMMA-PbO) nanocomposites increased with the increasing the films of thicknesses and the PbO nanoparticles concentration. While, the dielectric constant, and dielectric loss for (PMMA-PbO) nanocomposites are decreasing with the increase of frequency of the applied electric field, on the other hand, the A.C electrical conductivity increased with the increasing of the frequency.

Since these nanocomposites absorb well at high frequencies, they are used to attenuate radiation such as gamma rays. (PMMA-PbO) nanocomposites show good linear attenuation coefficients for gamma ray radiation.

Contents

List of Figures

List of Tables

List of Abbreviations

Abbreviation	Physical Meanings
PbO	Lead Oxide
FTIR	Fourier Transform Infrared
UV	Ultraviolet
SEM	Scanning Electron Microscope
OM	Optical Microscope
A.C	Alternating current
PMMA	Poly(methyl methacrylate)

List of Symbols

Symbols	Physical Meanings
$\sigma_{A.C}$	A.C electrical conductivity
I_A	Absorbed intensity of light
A	Absorption
α	Absorption coefficient
E_{act}	Activation energy
W	Angular frequency
μ	Attenuation coefficient
C	Capacitance
I_q	Capacitance current
ε	Complex dielectric constant
N	Complex refractive index
I_p	Conduction current
C.B	Conductive band
ε'	Dielectric constant
ε″	Dielectric loss
Tanδ	Dielectric loss tangent
k_0	Extinction coefficient
ε_2	Imaginary dielectric constant
Z	Impedance
I_o	Incident intensity of light
I_T	Intensity of transmittance
V_m	Maximum voltage
Eg^{opt}	Optical energy gap

C_p	Parallel capacitance
R_P	Parallel resistance
E_{ph}	Phonon energy
Z	Photon frequency
V	Potential exerted
ε_1	Real dielectric constant
n	Refractive index
t	Thickness
T_r	Transmittance
UV	Ultraviolet spectrum
C_o	Vacuum capacitor
ε_o	Vacuum permittivity
V.B	Valens band
C	Velocity of light
K	Wave vector
B	Width polar
N_o	Number of transmitted particles

Chapter One

Introduction & Literature Review

1.1 Introduction

Polymers are defined as macromolecules composed of one or more chemical units (monomers) that are repeated throughout a chain. Polymers are of profound interest to society and are replacing metals in diverse fields of life, which can be further modified according to modern applications. They are more desirable than traditional materials in such areas as packaging, construction, and medical applications.The processing of polymeric materials depends on applied heat and pressure etc… [1].

Today, it is possible to create polymers from different elements with almost any quality desired in an end product. Some polymers are similar to existing conventional materials but with greater economic values, some represent significant improvements over existing materials, and some can only be described as unique materials with characteristics unlike any previously known to man. Polymer materials can be produced in the form of solid plastics, fibers, elastomers, or foams. They may be hard or soft or maybe films, coatings, or adhesives. They can be made porous or nonporous or can melt with heat or set with heat. The possibilities are almost endless and their applications fascinating [2,3].

The polymer compound is a one-phase rigid multi-phase compound with separate polymer matrices in two or three dimensions. In addition, polymer compounds can be used as high-performance components, as the reinforcement properties differ considerably and are better than the matrix properties. Polymer composites have excellent mechanical strength and stiffness, and are corrosion resistant [4]. A particular feature of polymers is the possibility of linking together separate chains to form networks. Such cross-links can be introduced by copolymerizing a

monofunctional monomer such as styrene with a dysfunctional monomer such as divinylbenzene [5]. Polymers, such as polymethyl methacrylate, have excellent attention in many applications because of their unique properties:" low density, ability to form intricate shapes, and low manufacturing cost" [2].

1.2 Structure of polymer

The physical characteristics of polymer materials depend not only on molecular weight and shape but also on molecular structure. The different types of polymer chains, as shown in Figure (1-1) [6]:

1. Linear polymers: Van der Waals bonding between chains. Examples: polyethylene and nylon.
2. Branched polymers: chain packing efficiency is reduced compared to linear polymers - lower density.
3. Cross-linked polymers: chain is connected by covalent bonds. Often, it is achieved by adding atoms or molecules that form covalent links between chains. Many rubbers have this structure.
4. Network polymers: 3D networks made from trifunctional mers. Examples: epoxies and phenol-formaldehyde.

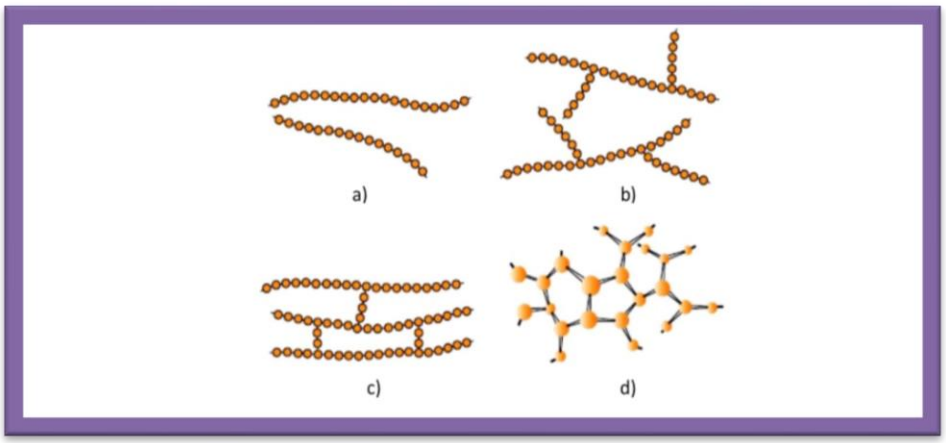

Figure (1-1): Polymer Chains

a) Linear polymers, b) Branched polymers , c) Cross-linked , and d) Network polymers [6].

1.3 Polymerization:

Polymerization is the process of transforming low molecular weight (monomers) to high molecular weight matters without making any change to the basic structure of molecules. Carothers (1940) and Flory (1953) divided polymerization processes into two groups [7]**:**

1.3.1 Additional polymerization

It is also called chain-growth polymerization. The bearer of the chain is an ion or a substance that is charged with a single electron called a free radical [8].

A free radical is formed by the decomposition of an unstable molecule of matter (initiator). It can react by opening the double bond to form another molecule that contains a single electron. In a very short time monomer molecules are added to the second chain, the process ends with the formation of two free radicals that eradicate each other, resulting in the formation of one molecule or more of the polymer. In this process, a polymer is formed in the first stages [8].

1.3.2 Condensation polymerization

It is also called step-growth polymerization. It takes place in compounds with low molecular weight, in this type of polymerization, two molecules that contain multi-functional groups react with each other, resulting in a bigger molecule that also contains multi-functional groups. In this process, a molecule of water may be eliminated. This process continues until the entire depletion of one of the reactants. In contrast with the additional polymerization, the polymer in the condensation polymerization is formed at the last stages of the polymerization process [9].

1.4 Thermal classification of polymers:

Polymers are classified according to the effect of temperature in to :

a. Thermoplastic polymers

The properties of these polymers are changed by the effect of temperature. When the temperature increases, they become flexible and sticky. By lowering the temperature, these polymers return to their original solid state. This is because the molecules in a thermoplastic polymer are connected by relatively weak intermolecular forces (Vander Vales forces). When heated, these molecules can slide over each other as in polystyrene, polyethylene, polypropylene and polyvinyl chloride, as shown in Figure (1-2 a) [10].

b. Thermoset polymers

These polymers are chemically changed when heated. Thermosets are usually three-dimensional networked polymers in which there is a high degree of cross-linking between polymer chains, as shown in Figure (1-2 b). After being heated, these polymers become insoluble, non-conductive of heat and electricity and hard because molecules of these polymers are connected by strong covalent chemical bonds. Phenol formaldehyde resin and urea-formaldehyde resin are examples of this type of polymer [11].

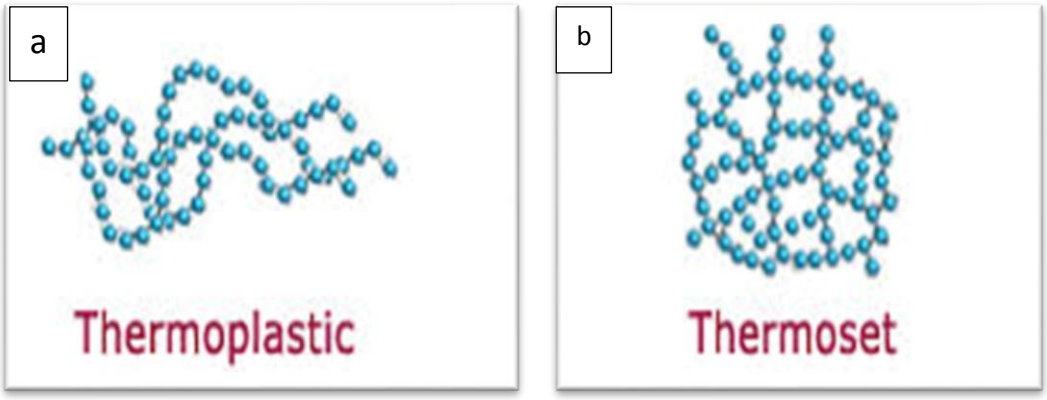

Figure (1-2): Schematic representation of (a) thermoplastic polymer,(b)thermosetting polymer [12].

1.5 Composite materials

The word composite in the term composite material signifies that two or more materials are combined on a macroscopic scale to form a useful third material. The key is the macroscopic examination of a material where the components can be identified by the naked eye. Different materials can be combined on a microscopic scale, such as in alloying of metals, but the resulting material is for all practical purposes, macroscopically homogeneous, the components cannot be distinguished by the naked eye and essentially acts together. The advantage of composite materials is that, if well designed, they usually exhibit the best qualities of their components, and often some qualities that neither constituent possesses [13], they are engineered materials made from two or more constituent materials, with significantly different physical or chemical properties, which remain separate and distinct on a macroscopic level within the finished structure [14]. Polymer matrix-ceramic filler composites receive increased attention due to their interesting electrical and electronic properties, integrated decoupling capacitors, angular acceleration accelerometers, acoustic emission sensors, and electronic packaging is some potential applications fields [15].

1.6 Nanomaterials:

A material with dimensions below "100 nm" they have at least one unique property that is different from the bulk material and the characteristics can be applied in different fields such as nanoelectronics, pharmaceutical, and cosmetics. Several methods have been studied in fabricating these nanostructures which include laser ablation, chemical vapor deposition (CVD) [16], and template-directed growth [17].

Nanomaterials can be classified according to different approaches such as; according to the X, Y, and Z dimensions, according to their

shape, and according to their composition. A nanomaterial is an object that has at least one dimension in the nanometer scale [18]. Nanomaterials are categorized according to their dimensions into four classes [19] :

1. Zero-dimension (quantum dot).
2. One-dimension (quantum wire).
3. Two-dimension (quantum well).
4. Three-dimension (bulk).

1.7 Nano composites

Nano composite polymers are defined as homogenous or heterogeneous, two-phase systems that consists of polymers and fillers with at least one dimension within the nano-range (1-100) nm. The fillers can be Nano fibers, two-dimensional clay platelets, one dimensional nanotube, or three-dimensional spherical particles. Polymers are the most popular materials used in the manufacturing of nanocomposites such as thermoplastics, thermosets or elastomers [20].

Over the past decades, polymer nanocomposites have drawn significant attention in both academia and industry, and they have become a crucial factor in the production of innovative advanced materials suitable for a range of uses, including electrical engineering [20]. Nano-composites are composed of synthetic and natural polymers, and nano materials, which refer to materials with nano sizes or are comprised from nano-sized building components [21]. The mechanical, electrical, thermal, electronic, and electro-chemical properties of nanocomposites can vary greatly from those of their component materials [22].

1.8 Materials Used in this Study

1.8.1 Poly(methyl methacrylate) (PMMA)

Poly (methyl methacrylate) is one of the earliest and best-known polymers. It is a significant and fascinating polymer due to its appealing physical and optical features, which determine its wide applicability. PMMA is a non-biodegradable polymer with good transparency, mechanical strength, less weight, and chemical resistance. Thermoplastic material with good tensile strength and hardness, and high rigidity. If it is polymerized between the float glass panels, it has a high shine on the surface [23]. Besides being polishable, it is weatherproof and resistant to weak acids and alkalis, non-polar solvents, fats, oils, and water without sacrificing its structural integrity. As a result of its outstanding light transmission and the fact that it can be colored to a high degree of saturation, (PMMA) is widely used in the lighting sector [24]. The PMMA (acrylic) polymer exhibits high levels of light transmission, making it an excellent choice for optical applications. PMMA enables more light to travel through it than glass or other polymers, allowing 92 % of light to pass through. Table (1.1) shows the most important properties of PMMA polymer. These plastics can be easily thermoformed without any loss of visual clarity compared to polystyrene and polyethylene [25]. (PMMA) has been successfully utilized to freeze enzymes, build micro-locked devices, precipitate minerals, and freeze proteins and DNA [26]. Figure (1.3) shows the chemical structure of the PMMA polymer's repeating unit.

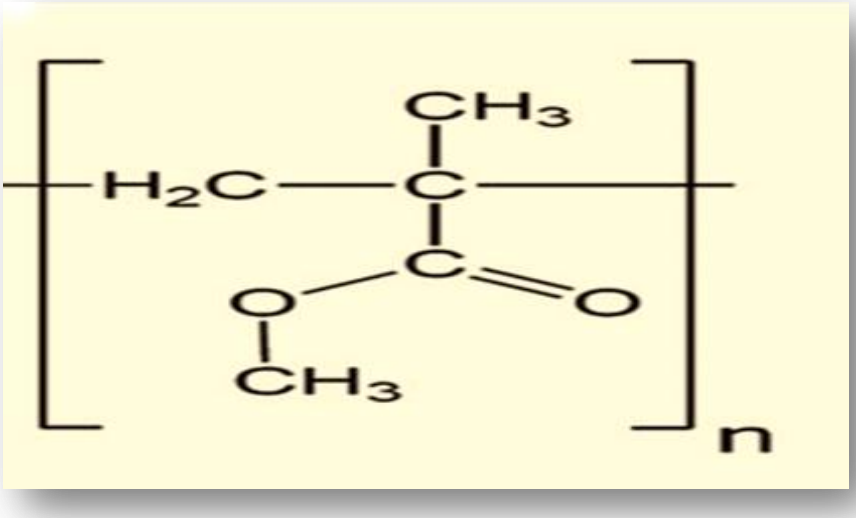

Figure (1.3): Chemical Structure of PMMA [27].

Table (1.1) : A most important characteristics of PMMA [28].

Parameters	PMMA
Chemical formula	$(C_5O_2H_8)_n$
T_g(°C)	106 °C
Refractive index	1.49
Density (g/cm^3)	1.2 g/cm^3
Melting point(°C)	160 °C

1.9 Nanomaterial used in this study

1.9.1 Lead Oxide (PbO):

Lead monoxides are TCOs (transparent conducting oxides) with the dielectric constant of ε =25.9 PbO was seen as a surface modification layer in inverted cells of the polymer solar. α-PbO is sufficiently applied in photovoltaic uses because of their low band gap, whereas β-PbOs are applicable as a surface modification layer for lowering work functions [29]. The orthorhombic β-PbOs or tetragonal α-PbOs are found to be essential industrial raw materials. Well known for its bright color good

photoconductivity and easy chemical conversion as a result, it has been widely used as the pigments for making coatings, paints and glasses, the key materials for fabricating electron tubes, television picture tubes and x-ray detectors and the raw materials for producing lead metal and its derivative [30]. The strong electro-chemical efficiency of PbO and its stability in the medium of acid have remarkably increased the amount of attention towards it in research [31]. The common properties of PbO are listed in Table (1.2).

Table 1.2: Physical and chemical properties of lead oxide [32].

Property	Value
Molecular formula	PbO
Density (g/cm^3)	11.34 (g/cm^3)
Melting temperature (T_m) ^oC	327.5 ^oC
Melting point	888 ^oC
Boiling point	1477 °C
Molecular Weight	223 g/mol
PH	Strong base

1.10 Literature Review:

P. P. Jeeju *et al.* in (2013) [33], prepared films of ZnO/PS/PMMA nanocomposites by using the spin coating technique to enhance the optical properties of these nanocomposites. They found that the ZnO/PS/PMMA nanocomposite films with 10 wt.% ZnO content exhibits shielding in the UV region and, high transparency in the visible region. They found these results indicated optical limiting type nonlinearity in the films due to two-photon absorption. They also found that the minimum transmittance of around 0.25 has been observed in the ZnO/PS/PMMA

nanocomposite films which is much lower compared to that in ZnO/PMMA and ZnO/PS nanocomposite films.

K. Al-Ammar *et al*. in (2013) [34], studied the optical properties of $CrCl_2$/PMMA composites, the samples were prepared with different concentrations of $CrCl_2$ and with different thicknesses. They found that the optical constants were increased and the forbidden energy gap was decreased when the particles of $CrCl_2$ increased inside the polymer.

W. A. Musa *et al*. in (2013) [35], studied the thickness effect on the optical constants of polymethacrylate (PMMA) doped by Potassium Iodide. They found that the transmission intensity decreases with increasing the film thickness, and the reflectance increases with the increasing film thickness. The dielectric constant (real and imaginary) was also found to be increasing with increasing the film thickness.

S. Sugumaran and C. S. Bellan in (2014) [36], studied the Al/PVA–TiO_2/Al and Al/PMMA–TiO_2/Al sandwich structures were prepared to study the dielectric behavior. The presence of metal–oxide (Ti–O) bond in the prepared films was confirmed by Fourier transform infrared spectroscopy. X-ray diffraction pattern indicated that the prepared films were predominantly amorphous in nature. Scanning electron micrographs showed a cluster of TiO_2 nanoparticles distributed over the film surface and also there were no cracks and pin holes on the surface. The transmittance of the films was above 80% in the visible region. The determined refractive index (n) values were between 1.6 and 2.3.

N. G. Hamed and M. Rahem in (2014) [37], studied the optical and electrical properties of Ag/PMMA composite, they prepared the samples as films with different concentrations by using the casting method. They found that there was a nonlinear proportion between the optical constants and the concentration ratio, which was attributed to their incompatibility.

Also, they found an increase in the absorption spectra with an increase in the silver concentration in Ag/PMMA composites, they refer it to the increase in localized states. They also found the best conductivity was at a 9%Ag ratio and the lowest receptivity.

B. H. Rabee and B. A. Al-Kareem in (2015) [38], studied the optical properties of (PMMA-CuO) nanocomposites by using the casting method for preparing these nanocomposites with different concentrations of CuO, they found that the absorption coefficient, extinction coefficient, refractive index, and real and imaginary dielectric constants of (PMMA/CuO) nanocomposites increased with the increasing of the copper oxide nanoparticles concentrations and the energy band gap of (PMMA/CuO) nanocomposites was decreased with the increase of the copper oxide nanoparticles concentrations.

R. T. Abdul Wahid *et al*. in (2016) [39], studied the structural and optical properties of (PVA-PbO) polyvinyl alcohol of solid polymer nanocomposites based on polyvinyl alcohol leads oxide. The results have shown that the refractive index and absorption coefficient of polyvinyl alcohol rose whenever the concentration of lead oxide nanoparticles increased, while the energy band gap was reduced with a rise in concentration.

P. Maji *et al*. in (2016) [40], studied the structural, dielectric, optical, and A.C conductivity properties of PMMA–ZrO_2 polymeric nanocomposite films. They prepared these films by the casting technique. They found by using XRD that the polymeric PMMA–ZrO_2 nanocomposite films appeared to a crystalline nature, by the UV–VIS spectroscopy they found that the nanocomposite films had highly visible with light transparency and high UV shielding efficiency, and the dielectric permittivity and dissipation factor decreased with frequency and increased with temperature. In addition, the values for dielectric

constant found relatively high at low frequency (100 Hz) they attributed it to the existence of interfacial polarization.

j. k. Ahmed *et al*. in (2019) [41], studied the interactions between poly (methyl methacrylate) (PMMA) and poly (vinyl alcohol) (PVA) biopolymers with the natural polymer chitosan showing a clear depression in the glass transition temperature (Tg) in both biopolymers except with 7% chitosan shows an elevation in the Tg of (PVA). This can explain due to the ability of both (PVA) and chitosan to make hydrogen bonding with each other while (PMMA) can only accept acidic hydrogen whilst (PVA) has the ability to accept and donate acidic hydrogen with chitosan. Thus Tg begins to increase. From Tg values calculation of the energy accompanied with the addition of chitosan to the polymers was done.

A. A. Abid *et al*. in (2020) [42], studied the polymer mixture of PVA-PVP-C. B (Carbon Black) nano-composites. The casting method was used to prepare these nanocomposites. Optical properties, FTIR, and optical microscope were examined as well. The absorbance of these nanocomposites increased with the rising rates of (C.B) nanomaterial concentrations. The energy bandgap of the nano-composites has decreased with the increase in carbon black (C.B) concentrations. These nanocomposites refractive index, absorption coefficient, extinction coefficient, and (real, imaginary) dielectric constants increased in proportion to the increase in carbon black concentrations.

A. A. Abid *et al*. in (2021) [43], studied the polymer blend (PVA-PVP)-Carbon black (C.B) nanocomposites. The (PVA-PVP-C.B) nanocomposites were prepared by casting method. The optical microscope, FTIR, and electrical properties had been studied. The constant of dielectric with the dielectric loss of the samples were reduced

with increasing the value of frequency during the application of electric field, while an increase in the A.C electrical conductivity results existed with the rising the value of the frequency. The electrical conductivity (A.C), dielectric loss, and constant of all the samples were increased with the increase of the carbon black concentrations.

M. S. Toman and S. H. Al-nesrawy in (2021) [44], studied new fabrication (PVA-CMC-PbO) nanocomposites structural and electrical properties. They found that –the dielectric constant, dielectric loss and the A.C electrical conductivity for (PVA-CMC-PbO) nanocomposites are increasing with the increase of the lead oxide rate. The dielectric loss and dielectric constant are decreasing, with the increase of frequency.

M. A. Kadhim and E. Al-Bermany in (2021) [45], studied the mixed PMMA- dissolved in dimethylformamide (DMF) with PVA dissolved in distilled water (DW) and DMF. New (PMMA-DMF)-(PVA-DW-DMF)/GO nanocomposite was successfully fabricated with various loading ratios of GO nanosheets for the first time. Several factors were applied to get fine desperation and homogeneous using the acoustic-solution casting method. Optical Microscope, Fourier-transform infrared spectroscopy, X-ray diffraction, and UV–visible spectrophotometer were applied to investigate the structure and optical properties of the PMMA-PVA-GO nanocomposite. The OM images confirmed the fine homogenous matrix and GO distribution in the nanocomposites. These results could grow for better and wide applications such as radiation shielding, specific optoelectronic applications, and filters ultraviolet also could use in landfilling the chemical, nuclear, and radioactive waste.

O. B. Fadil and A. Hashim in (2022) [46], studied the fabrication and tailored optical characteristics of CeO_2/SiO_2 Nanostructures doped PMMA for electronics and optics fields. They discovered that the

absorbance of PMMA at the wavelength (λ) = 240 nm rose about 33.5% and transmission decreased about 53.7% when the CeO_2/SiO_2 NPs content reached (5.4 wt.%). The energy band gap of PMMA dropped from 4.14 eV for pure PMMA to 2.14 eV when the concentration of CeO_2/SiO_2 nanoparticles (NPs) reached (5.4 wt. %). The optical parameters of PMMA, including refractive index, optical conductivity, and dielectric constants, increased with the addition of CeO_2/SiO_2 NPs.

1.11 The Aims of the Study:

The aims of this study can be summarized in the following points:

1. Preparing (PMMA-PbO) nanocomposites.
2. Study of the structural, optical, and alternating current electrical characteristics of (PMMA-PbO) nanocomposites.
3. Studying the attenuation of gamma rays by (PMMA-PbO) nanocomposites.

Chapter Two

Theoretical Part

2.1 Introduction:

This chapter involves a general description of the theoretical part of this study, physical concepts, scientific clarification, relationships, and laws used to interpret the study results of structural, optical, and electrical properties. Structural properties used in this study are given by (optical microscopic, Fourier Transform Infrared spectrometer (FTIR), Scanning Electron Microscope (SEM),optical properties of nanocomposite (the optical constants, fundamental absorption edge, electronic transitions), electrical properties (dielectric loss, dielectric constant, A.C electrical conductivity). This explanation can be considered as a gateway to access scientific knowledge of polymer nanocomposites.

2.2 Morphology and Structural Properties

2.2.1 Optical Microscope

A compound optical microscope is an optical instrument that magnifies an object (or specimen) and transmits the magnified image to the retina of the eye or to an imaging device through visible light, perhaps produced in its current form during the seventeenth century. While many elaborate designs strive to increase the resolution and contrast between samples, basic optical microscopes are sometimes rather simple. Historically, optical microscopes were simple to construct and remain popular owing to their use of visible light, which allowed the naked eye to observe materials directly [47]. Microscopy would be most frequently used to examine microscopic light-diffracting specimens such as diatoms, bacteria, and bacterial flagella, isolated organelles, and polymers such as flagella, cilia, microtubules, and actin filaments, as well as silver and gold grains in histologically labeled cells and tissues. It is crucial to have an adequate quantity of scattering elements in the specimen, since an excess

may obscure fine detail by brightening the backdrop [48], as shown in Figure (2-1).

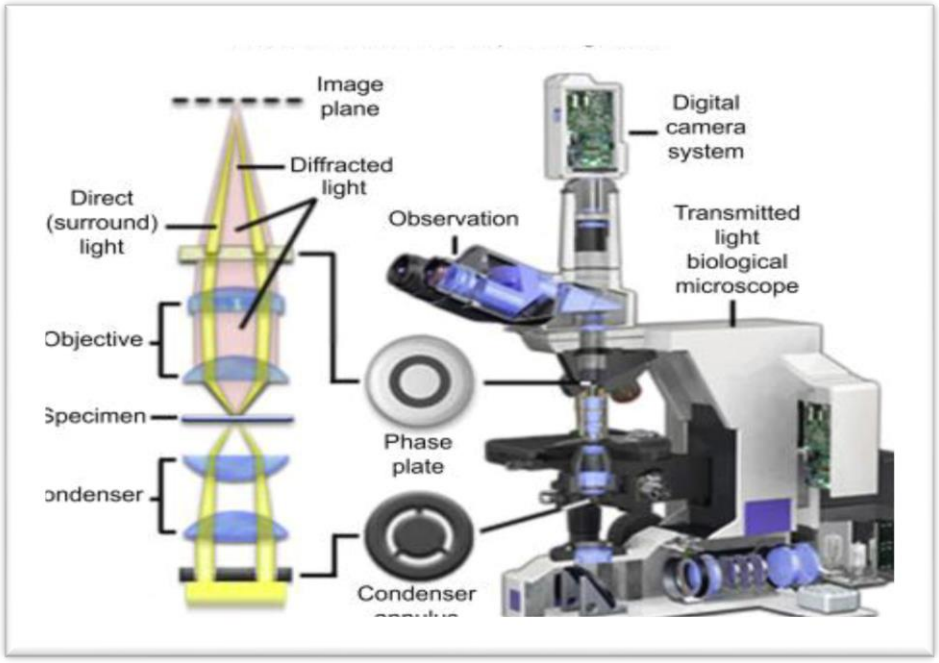

Figure (2-1). Optical Microscope [49].

2.2.2 Fourier Transform Infrared Spectrometer (FTIR)

The Fourier Transform Infrared (FTIR) Spectroscopy is a non-destructive chemical characterization method. This spectral region is classified into three regions far-infrared, near-infrared and, mid-infrared which are between (4~400) cm^{-1}, between (400~4,000) cm^{-1} and lastly, between (4,000~14,000) cm^{-1}, respectively. FTIR spectroscopy is a vibrational spectroscopic method that can be used for the optical study of molecular shifts. The allowable existence of this technology relies on the identification of vibration in the sample by the chemical functional group. Wherever an interaction takes place between infrared light and matter, the chemical bonds will stretch. Infrared radiation is absorbed by the chemical functional group at a specific wavenumber frequency, independent of the rest of the molecule composition [50].

The FTIR spectroscopy form is advantageous in several advanced areas, such as microanalysis (whereby higher sensitivity is needed), in the

dark, solid state samples or analysis of aqueous solutions that involve the focus on quantitative assessment, and in studies whereby study time is a limiting factor, such as in quality control measurements or processing [51], as shown in Figure (2-2).Various spectroscopic techniques are applied in studying the different samples. However, FT-IR spectrometers are becoming increasingly common because they deliver, speed precision and sensitivity which were previously difficult to obtain through dispersive spectrometer wavelengths. This technicality enables micro samples to be analyzed rapidly to reach for nano-gram levels. Given that FT-IR is a crucial tool for solving issues within various fields of study, it still needs more research, as its concepts vary from those dispersive spectroscopy techniques which use interferometers within spectrometers [52].

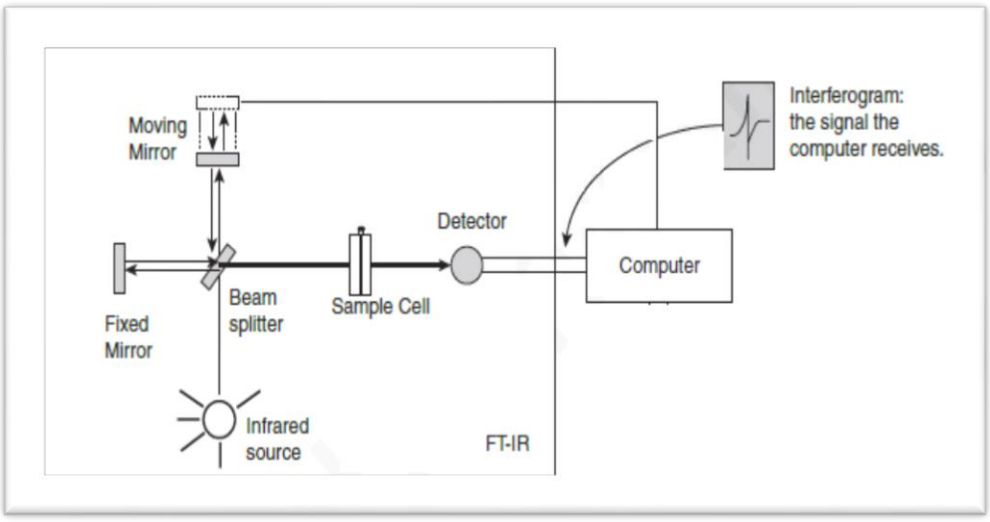

Figure (2-2). Schematic Illustration of the FTIR System [53].

2.2.3 Scanning Electron Microscope.

One of the most significant advancements in the field of electron beam technology throughout the twentieth century was the scanning electron microscope. Since the early 1960s, when the first commercial

equipment was introduced, the design of the scanning electron microscope has been constantly evolving and improving [54]. Electron microscopes operate on the same fundamental principles as light microscopes but magnify objects by focusing beams of powerful electrons rather than photons [55], as shown in Figure (2-3).

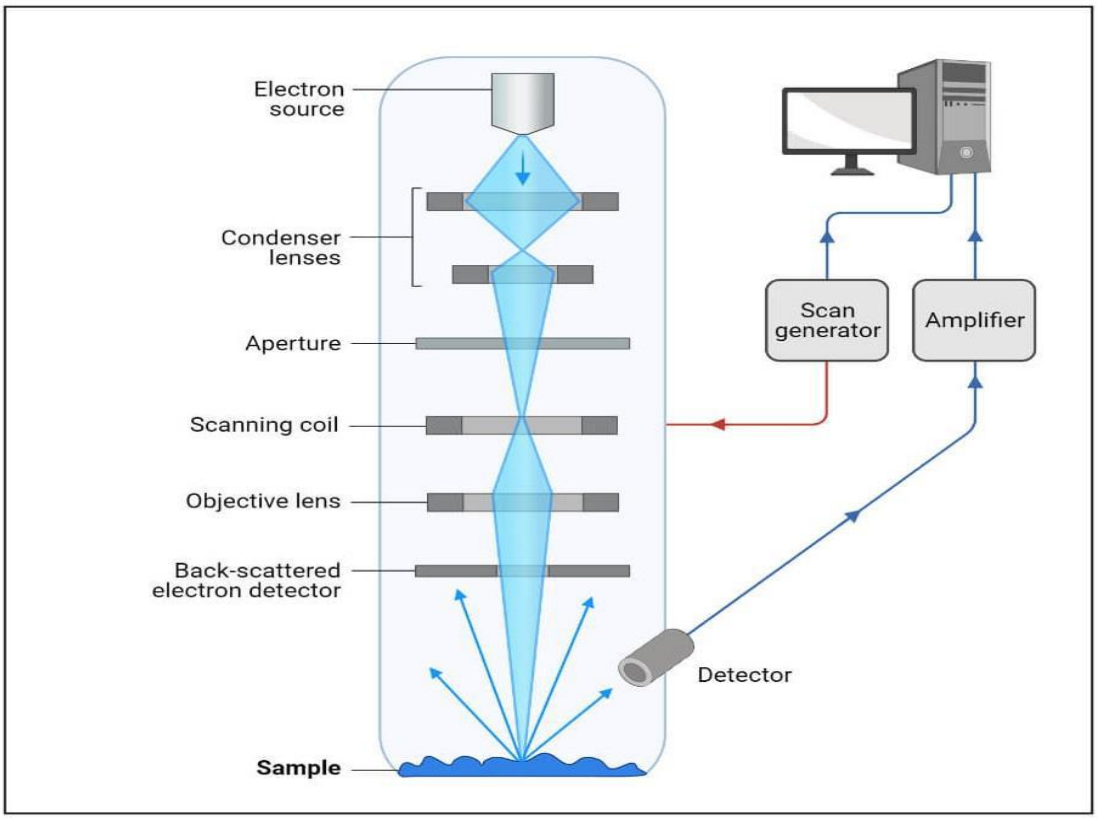

Figure (2-3). Ray Diagram for a system of SEM [56].

2.3 Optical Properties:

The optical absorption spectroscopy technique is a very efficient method for examining electronic changes induced by light. Additionally, they investigate the energy gap and band structure of crystalline and amorphous materials theoretically. According to this idea, photons with an energy level greater than the band gap energy are collected by the absorption and transition of ultraviolet and visible light [57,58].

In recent years, the search for optical properties has increased due to their use in integrated optics, such as optical data storage and optical

information. Research on the optical and electrical properties of polymers has also received a great deal of interest in the light of their application in similar apparatus. Electrical conduction in polymers was examined with a view to understanding the characteristic features of the load transport prevailing in these materials, whereas optical properties are developed to enhance reflective and anti-reflective interference and polarization properties [59].

2.3.1 Absorbance (A)

Absorbance is defined as the intensity of the absorbed light (I_A) by the materials to the incident intensity of light (I_o) as a ratio, which is given in the following equation [60].

$$A = \frac{I_A}{I_\circ} \quad \text{.....(2.1)}$$

2.3.2 Transmittance (T_r)

The intensity of transmitted rays from the film (I_T) over the intensity of incident rays on the film (I_o) is called the transmittance (T_r) and can be obtained as follows [61].

$$T_r = I_T / I_o \quad \text{.....(2.2)}$$

2.3.3 The absorption coefficient (α)

An absorption coefficient can be described as the ratio at which incoming radiation decreases proportionately to the unit length of the medium in the direction of wave propagation [62]. It depends on the photon energy (hυ) Photon energy created by Planck's relationship [59]:

$$E = h\upsilon = \frac{hc}{\lambda} \quad \text{..... (2.3)}$$

Where (c) represents the speed of light, and (λ) represents the wavelength of light. The absorption coefficient can be calculated by using Lambert's law which states that the absorbance of a material sample is directly

proportional to its thickness (path length) (t), and it can be written as the following [63]:

$$\frac{I}{I_\circ} = e^{-\alpha t} \quad \text{..... (2.4)}$$

Where $\frac{I}{I_\circ}$ the ratio of the transmittance intensity of the incident wave to the incident intensity of the same wave which represents the transmittance of the electromagnetic wave (T) and because the absorbance (A) is written as A= Log ($\frac{I}{I_\circ}$), then by doing some mathematical steps the absorption coefficient can be written as [63]:

$$\alpha = \frac{2.303}{t}\text{A} \quad \text{.....(2.5)}$$

Where: α is the absorption coefficient.

2.3.4 Fundamental Absorption Edge

The fundamental absorption edge can be defined as the rapid increasing in absorbance when absorbed energy radiation is almost equal to the band energy gap; therefore, the fundamental absorption edge represents the less difference in the energy between the up point in the valance band to the bottom point in conduction band [64].

2.3.5 Absorption Regions

Absorption regions can be classified into three regions, as seen in Figure (2-4):

A) High absorption region

In this area, the absorption coefficient is about ($\alpha \geq 10^4$ cm^{-1}) [65].

B) Exponential region

The value of absorption coefficient (α) is equal to ($1\ cm^{-1} < \alpha < 10^4\ cm^{-1}$). It indicates the transition from the extended level at the top of the valence band towards the localized level at the conductive band and vice versa, from the local level at towards the extended level at the bottom from conductive band [66].

C) Low absorption region

The absorption coefficient (α) in this region is very small, it is about ($\alpha<1cm^{-1}$). The transition happens in this region because of state density inside space motion resulted from faults structural [67].

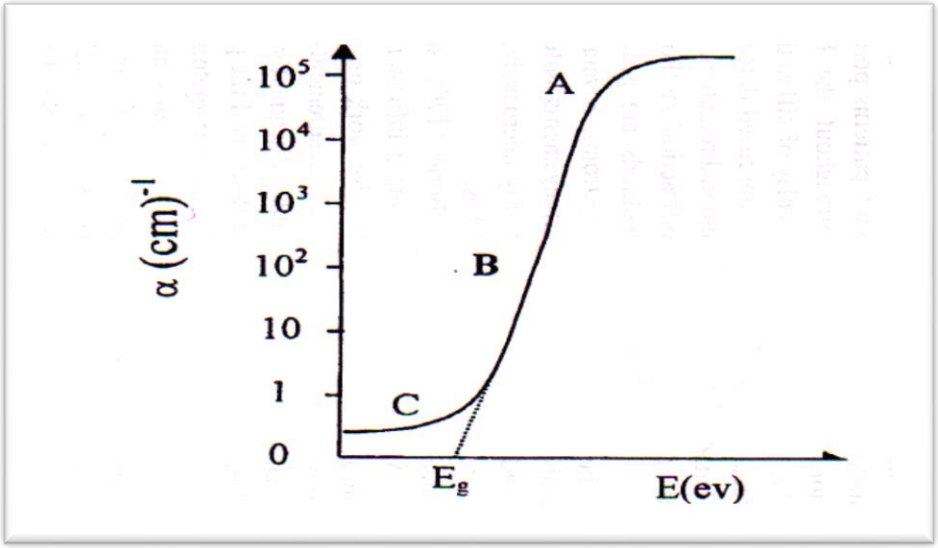

Figure (2.4): The absorption regions [68].

2.3.6 Electronic Transitions

The electronic transitions can be classified basically into two types:

2.3.6.1 Direct Transition

This transition occurs in semiconductors when the bottom of the conduction band (C.B.) is exactly over the top of the valence band (V.B.) indicating that they have the same wave vector value, i.e. Δ K=0; absorption occurs in this state when ($h\upsilon = E_g^{opt}$). The conservation of energy and momentum was needed for this transition form [69]. Direct transitions are classified into two kinds:

A- Direct Allowed Transition :

This transition happens from the top points in the valance band and the bottom point in the conduction band [70], as shown in Figure (2-5 a).

B- Direct Forbidden Transitions:

This transition happens from the near top points of the valance band and the bottom points of the conductive band, as shown in Figure (2-5 b). The absorption coefficient for this transition type is given by [71]:

$\alpha h\upsilon = B\,(h\upsilon - E_g^{opt})^r$ ……(2.6)

Where: E_g^{opt}. the energy gap between direct transition.

B: constant depended on the type of material.

r: exponential constant, its value depended on the type of transition,

r =1/2 for the allowed direct transition.

r =3/2 for the forbidden direct transition.

2.3.6.2. Indirect Transitions

As for the electronic optical indirect transition, the bottom of the conduction band and the top of the valance band are in various regions of space (k). This type of transformation happens with the aid of the phonon to maintain the motion arising from variation in the electron wave vector. Two types of indirect transition exist, namely whenever the transition is between the top point of the valance band and the lower point of the conduction band, which is located in the various regions of the space (k) called allowed indirect transition as shown in Figure (2-5 c), and when these transitions happen between near points in the top of valance band and near points in the bottom of a conductive band called forbidden indirect transitions, as shown in Figure (2-5 d) [72]. As seen in Figure (2-5), the coefficient of absorption for a transition with phonon absorption can be obtained through the following equation:

$\alpha h\nu = B(h\nu - Eg^{opt} \pm E_{ph})^r$…… (2.7)

Where (E_{ph}) is the energy of phonon. The value is (-) when the phonon is absorbed, whereas it is (+) in case the phonon is emitted. The value of (r) is (2) and (3) for the allowed and forbidden indirect transitions, respectively.

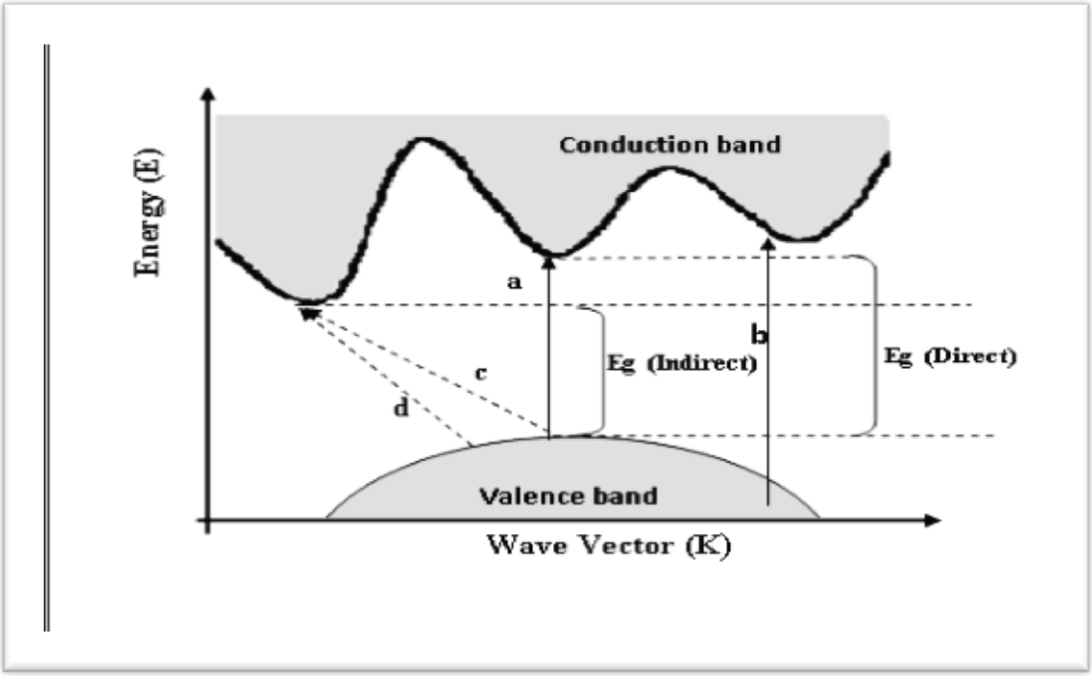

Figure (2-5): The Electronic transitions types of (a) Allowed direct, (b) Forbidden direct transition, (c) Allowed indirect, and (d) Forbidden indirect transitions [73].

2.3.7 The refractive index (n)

It is the ratio of light speed in a vacuum to its speed in a medium. This index shows how far a matter is affected by electromagnetic waves. It can be expressed by the following equation [74]:

$n = c/v$ …… (2.8)

where (n) is the refraction index, (c) is the light speed in a vacuum, and (v) is the light speed in the matter. The reflectance (R) was calculated from the transmission (T) and absorbance (A) values through the following equation [75]:

$R+T+A=1$ …….. (2.9)

The refractive index (n) can be calculated using the following equation [76].

$$n = \sqrt{4R - \frac{k^2}{(R-1)^2}} - \frac{(R+1)}{(R-1)} \ldots\ldots\ldots\ldots\ldots\ldots\ldots\ldots\ldots\ldots\ldots\ldots\ldots\ldots (2.10)$$

2.3.8 Extinction Coefficient (k_o)

The extinction coefficient (K_o) presents the amount of attenuation of the electromagnetic wave that passes through a material. Its value is determined by the density of the free electrons within the material and its structure, and expresses by the following relationship [77]:

$k_o = \alpha\lambda/4\pi$ ……(2.11)

Where (k) is the extinction coefficient, and (λ) is the wavelength of the incident light.

2.3.9 The Dielectric Constant (ε)

The dielectric constant demonstrates matter's polarization capability; it may react exceedingly poorly to different frequencies, and electronic polarity dominates other forms of polarization at optical frequencies represented by light waves, both real and imaginary parts of dielectric constants (ε_1, and ε_2) are calculated as follows [78]:

$\varepsilon_1 = (n^2 - k^2)$ …… (2.12)

$\varepsilon_2 = (2nk)$ ……... ……(2.13)

2.4 Electrical Properties

The electrical properties of a material are determined not only by the chemical composition but also by the arrangement of atoms in the solid, and the existence of defects when giving rise to the electron states in the energy gap which influence the electrical properties of a material. This defect can be reduced by many processes such as the annealing process [79]. Polymers are not entirely free of conduction mechanisms, a limited amount of charge carriers may have low-level conduction, and basically, insulating polymers may take a range of types. Conduction is very often caused by impurities that involve low concentrations of charge carriers that take form of electrons or ions [80]. Materials can be classified

according to their conductivity to insulators, conductors, semiconductors, and superconductors [76], whose conductivity ranges are 10^{-18}–10^{-8} (Ω .cm) $^{-1}$, 10^{-8}–10^{3} (Ω.cm)$^{-1}$, over 10^{3}–10^{8} (Ω .cm) $^{-1}$, and 10^{8}–10^{20}(Ω .cm)$^{-1}$, respectively [81]. Figure (2-6) described the conductivity of materials. To understand the electrical properties of the matter and how electrical conductivity takes place, it is necessary to know more about the energy levels of atom and the electronic distribution in these levels of energy gap in metals, semiconductors, and insulators electrons closer to the nucleus closely are connected to the atom. The more electrons are distanced from the nucleus, and the less is the connection of electrons to the nucleus. Consequently, an electron that occupies the orbital, which is the most distant from the nucleus, is the least connected to the nucleus. These electrons are called valence electrons. Valence electrons are distributed among many levels of energy, which are called valence band [82].

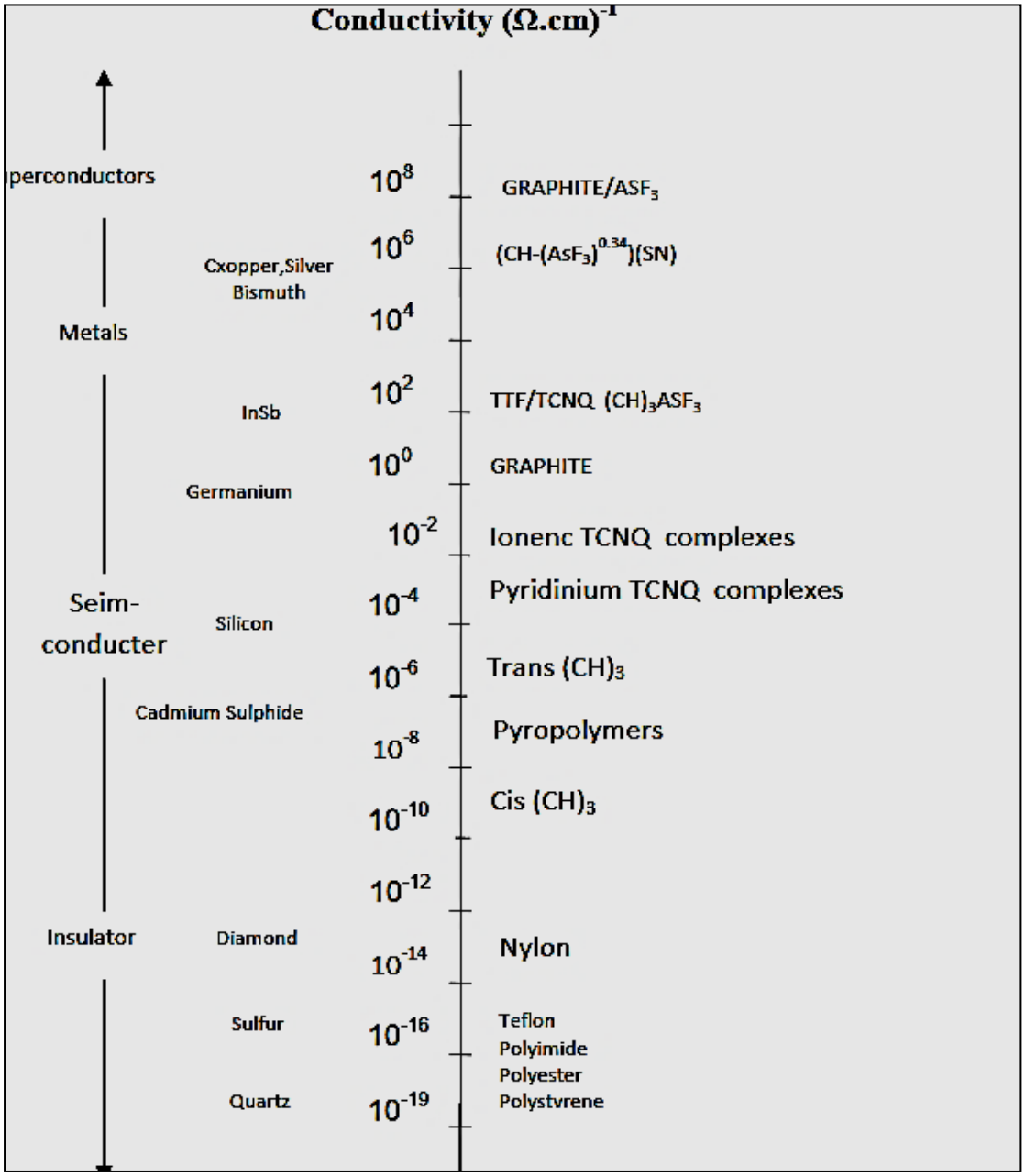

Figure (2-6): The Classification of Material Conductivity [83].

2.4.1 The A.C electrical conductivity

A.C conductivity affects the frequency of the electrical field [84]. Dielectric spectroscopy is based on the calculation of current and voltage phases and the amplitude A.C system. It is commonly used for the study of dielectric properties of polymers e.g. (ε', and tanδ) [85]. The electrical conductivity of isolation polymer materials can be improved through adding certain conductive fillers [86]. The dielectric constant is the ratio

of a condenser's capacitance with an insulator material between its conductive plates to the capacitance of a condenser of the same size with vacuum between its plates. Its value varies from material to material based on the amount of polarization that occurs in the material [87].

When an alternating potential $V = V_m e^{i\omega t}$ [87] is applied through a capacitor (C) loaded with an insulator, the current going through the capacitor will precede the potential by $\pi/2$ [88] :

$$I = j\omega c v_m \qquad \ldots\ldots. (2.14)$$

Where (**ω**) is the applied angular frequency of the filed **(ω=2πf)**, **(j)** refers to the number of imaginary and is equal to $\sqrt{-1}$, **(C)** is the capacitance of a capacitor, and **(V_m)** is the highest voltage. The angle between electric current and voltage is less than π/2, as seen in Figure (2-7). The sum of the conduction current (I_p) is assumed to be electric current. This is in the same phase with voltage, whereas the capacitates current (I_q) is with the phase variation (π/2). The current can be obtained through the equation below:

$$I = I_P + jI_q \qquad \ldots\ldots. (2.15)$$

The capacitance of a condenser consisting of two parallel plates can be defined through the following equation [89]:

$$C = \varepsilon\varepsilon_o \frac{A_r}{d} \qquad \ldots\ldots. (2.16)$$

where (A_r) is the area, and (d) is the thickness.

By substituting equation (2.16) in (2.14), the following relation is obtained:

$$I = j\ \omega\ \varepsilon\ \varepsilon_o V\ A_r/d \qquad \ldots\ldots(2.17)$$

The dielectric constant is then viewed as a complex quantity (ε). The difference of the real and imaginary components of the complex dielectric constant is defined as follows [90]:

$$\varepsilon = \varepsilon' - j\,\varepsilon'' \qquad \ldots\ldots(2.18)$$

Where: ε" is the dielectric loss.So,get:

$$I = j\,\omega\varepsilon_o \frac{A_r}{d} (\varepsilon' - j\,\varepsilon'')\,V \qquad \ldots\ldots(2.19)$$

By comparing equation (2.19) to (2.15), the following can be obtained:

$$I_p = \omega\varepsilon_o\,\varepsilon''\,\frac{A_r}{d}\,V \qquad \ldots\ldots.(2.20)$$

$$I_q = \omega\varepsilon_o\,\varepsilon'\,\frac{A_r}{d}\,V \qquad \ldots\ldots.(2.21)$$

Figure (2.7) shows that the loss factor (tanδ) is [91]:

$$\tan\delta = I_p / I_q = \varepsilon''/\varepsilon' \qquad \ldots\ldots(2.22)$$

The capacitor can be represented by an ideal capacitor connected in parallel with a resistance R_P at low frequencies, so [88]:

$$I = I_p + jI_q = \frac{V}{R_P} + j\,\omega C_p\,V \qquad \ldots\ldots(2.23)$$

After that, the impedance z is determined by:

$$\frac{1}{Z} = \frac{1}{R_P} + j\,\omega\,C_p \qquad \ldots\ldots(2.24)$$

From equations (2.20), (2.21) and (2.23), one can write :

$$R_P = d / \omega A_r \varepsilon_o\,\varepsilon'' \qquad \ldots\ldots(2.25)$$

$$\varepsilon'' = 1 / \omega\,R_P\,C_o \qquad \ldots\ldots(2.26)$$

$$C_P = \varepsilon_o\,\varepsilon'\,A_r\,/d \qquad \ldots\ldots(2.27)$$

$$\varepsilon' = C_P / C_o \qquad \ldots\ldots(2.28)$$

The dissipated power in the insulator is represented by the existence of alternating potential as a function of the alternating conductivity, as explained in the following equation [92]:

$$\sigma_{A.C} = \omega \varepsilon_0 \varepsilon'' \quad \ldots\ldots (2.29)$$

$\sigma_{A.C}$ represents the measurement of the temperature produced by the insulation material arising from the vibration of the charges or rotation of the dipoles in their positions. This is the result of the alternation of the field [93].

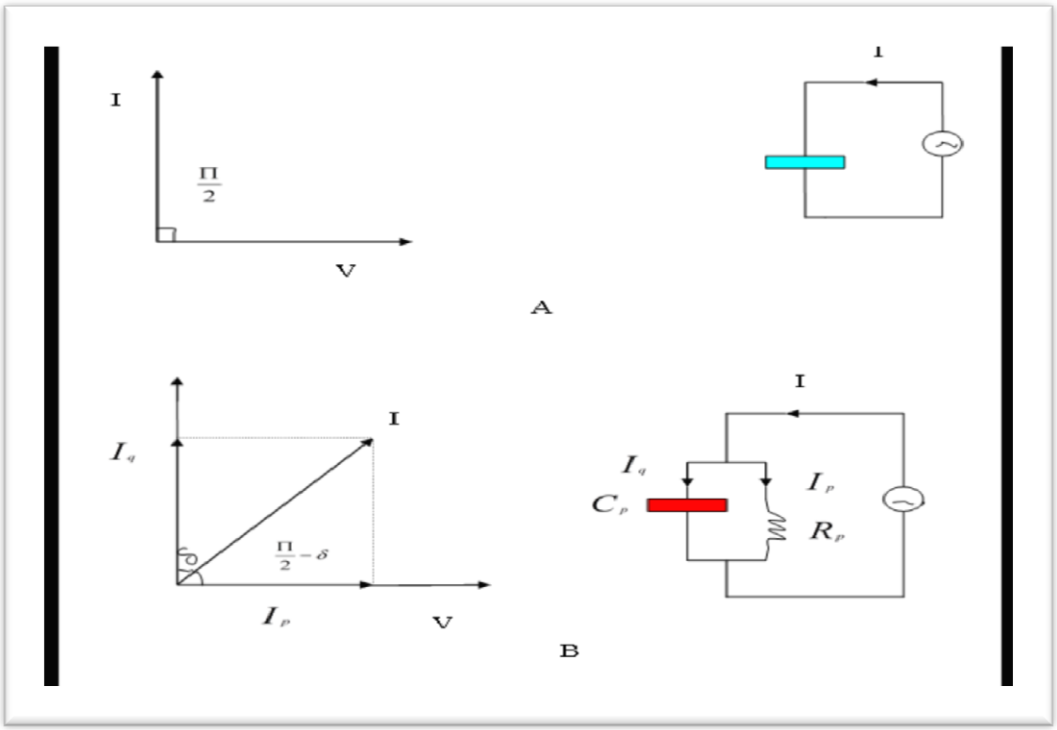

Figure (2.7): The circuit equivalent to a non-ideal capacitor [94].

2.6 Gamma ray shielding application

The advent of nanocomposites has contributed to developing a novel generation of nanocomposite materials that have different approaches in engineering, military industrialization, and medicine [95]. Industrial, science, and technological instruments and communication

techniques have been used on a comprehensive scale [96]. However, electro-magnetic interference remains a big concern as it decreases the life and performance of the instruments [97]. A sufficient number of studies have been conducted on the effects rays of gamma radiation produced by gamma sources, nuclear reactors, and even nuclear medicine on non-and living systems. High density materials composed of high-atom-number elements, such as lead or tungsten are the most effective shields for gamma-ray attenuation [98]. Interference electromagnetic shielding is the process in which electromagnetic radiation is absorbed or reflected by a material that acts as a barrier to radiation penetration through a shield [99].

With the use of active gamma ray isotopes in industry, agriculture, and medicine, researching the attenuation index of different materials has become significant both biologically and technologically [100]. The following equation shows the properties of the radiation attenuation:

$$N = N_o \exp(-\mu t) \qquad \ldots\ldots\ (2.30)$$

Where (N_o) represents the number of radiation particles counted at a given time. The period shall be without any absorber. (μ) is the attenuation coefficient of gamma radiation. (N) is the amount of counted radiation particles at the same time, with the thickness of the sampled [101].

Chapter Three

Experimental Part

3.1 Introduction:

This chapter discusses the processes involved in the preparation of samples, the use of instruments, and measurement methodologies. A general description of the materials (Polymethyl methacrylate (PMMA) and lead oxide (PbO)). This study makes use of a variety of microscopy methods, including optical microscopy, Fourier Transform Infrared (FTIR), and scanning electron microscopy (SEM), as well as pictures and schematics of several electrical circuits. Additionally, it comprises the use of gamma ray shielding.

3.2 The Utilized Materials

3.2.1 Poly (methyl methacrylate) (PMMA)

The polymer was used as granular form and was obtained from Apha Co, India (5000 M.W) with high purity (99.99 %).

3.2.2 Lead oxide nanoparticles (PbO) As Additive nanomaterial

Lead oxide (PbO) was used as a powder with particle average diameter (66) nm from EPRUI USA company with high purity (99.9%).

3.3 Preparation of (PMMA-PbO) Nanocomposites:

The following method is used to produce the (PMMA-PbO) nanocomposites , as shown in Figure (3.1):

1. The nanocomposites were prepared by dissolving PMMA in 30 ml of chloroform and mixing the material with a magnetic stirrer to create a more uniform solution at room temperature.

2. The PbO nanoparticles were added to poly(methyl methacrylate) in various weight percentages (0,1, 2, and 3) wt.%, as shown in Table (3-1) and stirred for 1 hour to achieve a more uniform solution.
3. Placing the mixture in a template (a 9cm diameter Petri dish) was well washed with distilled water many times.
4. The casting method is used to produce the nanocomposites on the template Petri dishes, which are then allowed to dry (7 days).
5. Micrometer was used to determine the thickness of the samples, and found to be within (60, 120, 220) μm.
6. Finally, the samples are ready for the procedure than necessary measurements.

Table (3-1): Weight percentages for (PMMA-PbO) nanocomposites.

PMMA(gm)	PbO (gm)
1	0
0.99	0.01
0.98	0.02
0.97	0.03

To obtain different thicknesses of the prepared films, the amount of polymer added to the nanomaterial is doubled and then tripled.

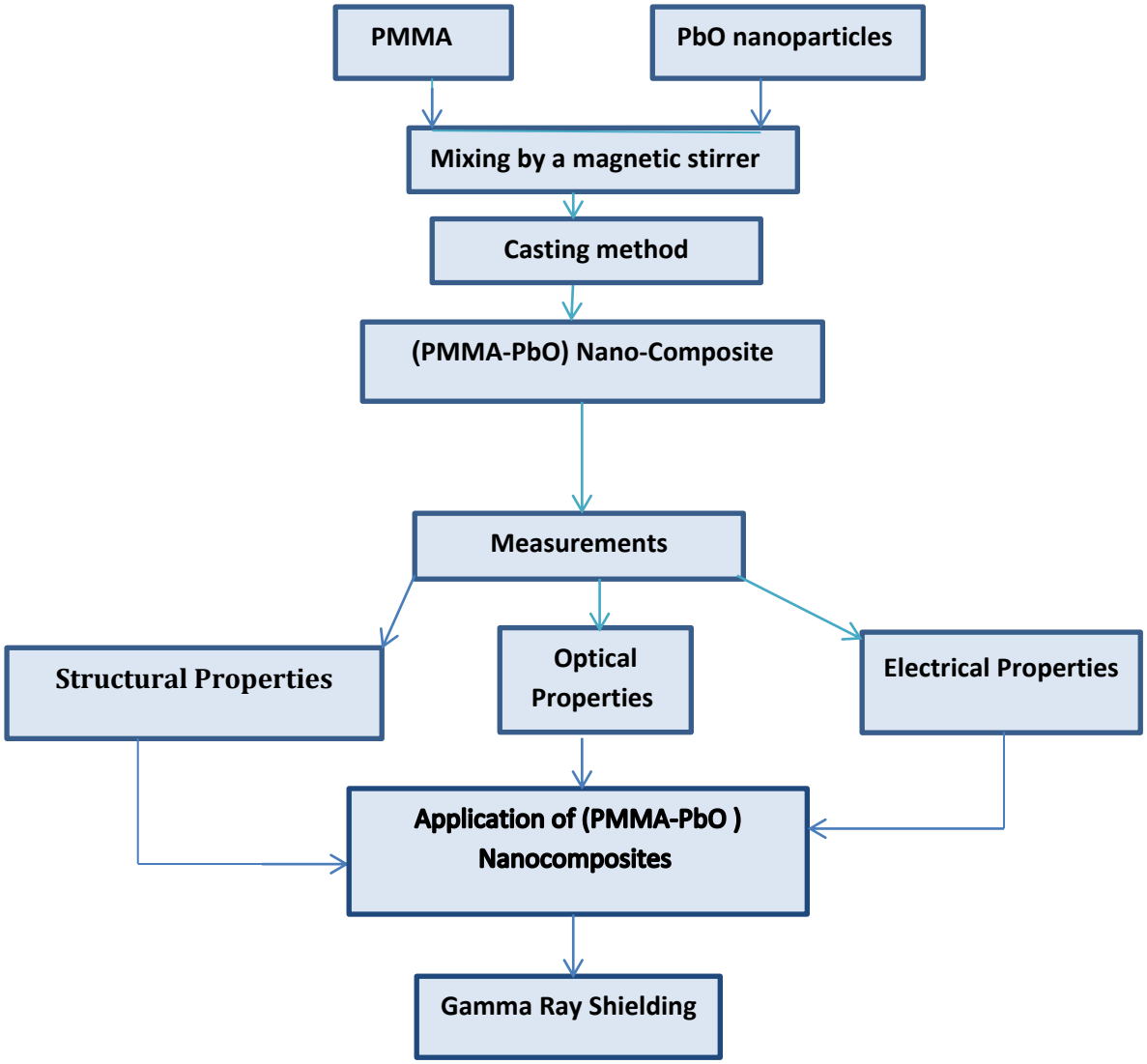

Figure (3.1): Scheme of Experimental Part

3.4 Structural Properties for (PMMA-PbO) nanocomposites

3.4.1 Optical Microscope (OM)

The sample of (PMMA-PbO) nanocomposites is examined by using the optical microscope, which is supplied from Olympus name (Toup View) type (Nikon -73346) and equipped with light intensity automatic controlled camera. Under magnification (10x) , this measurement was

implemented in University of Babylon / College of Education for Pure Sciences , Department of Physics.

3.4.2 FTIR Spectral Characterization

FTIR spectra were recorded by FTIR (Bruker company, German origin, type vertex -70). The considered wavenumber range is (4000-1000) cm^{-1}. This inspection was conducted at the University of Babylon /College of Education for Pure Sciences.

3.4.3 Electron Scanning Microscope (SEM)

SEM is an electron microscope that employs a high-energy electron beam to take raster scan images of the sample surface. Following sample preparation, the part of each sample with dimensions (5 mm x 10 mm) was cut and pleased into the SEM sample holder for examination. The surface morphology of (PMMA-PbO) composites is observed using (INSPEC F50 FE-SEM. fei company, made in Netherlands) used SEM is existent at the ALKHORY COMPANY SEM LAB-BAGHDAD-IRAQ.

3.5 Optical Properties Measurements

The optical characteristics of films of (PMMA-PbO) nanocomposites were determined using a double beam spectrophotometer (Shimadzu, UV-18000A) operating at wavelengths (200-1100) nm. This inspection was conducted at the University of Babylon /College of Education for Pure Sciences.

3.6 A.C Electrical Conductivity of (PMMA-PbO) Nanocomposites.

A.C Electrical Conductivity was determined at the University of Babylon/College of Education for Pure Sciences. Using (LCR) meter type HIOKI 3532-50 LCR Hi TESTER (Japan). The dispersion factor and capacitance of all samples were determined electronically at a frequency

between (100HZ - 6MHZ) at room temperature. These variables were used to compute the dielectric constant, dielectric loss, and conductivity.

3.7 Gamma Ray Shielding Application Measurements of Nanocomposites

Gamma ray shielding measurements of (PMMA-PbO) nanocomposites have been performed to examine attenuation properties of gamma rays for the specimens with various concentrations of (PbO) nanoparticles and different thicknesses. Test specimens with varying concentrations and thicknesses were ordered in front of the parallel beam emanating from the gamma ray exporter (Cs-137). The nanocomposite (PMMA-PbO) sample is placed at a distance of 1 cm from the gamma ray exporter and for one minute. The emitted gamma ray influxes through the specimens are determined by the Geiger counter which used for an estimate the linear attenuation coefficients.

Chapter Four

Results, and Discussions

4.1 Introduction

This chapter showed the results of the study and discussion the results; structural, optical, and A.C electrical measurements were discussed in this chapter. The effect of the thickness of films and the effects of nanoparticle additive (PbO) were studied by optical microscope, Fourier Transform Infrared Spectrometer (FTIR).

4 .2 Structural Properties of (PMMA-PbO) nanocomposites.

4.2.1 The Optical Microscope (OM)

The OM images of the pure PMMA polymer surface and its nanocomposites film at magnification strength (10X)with different concentrations of PbO, and different thicknesses of films were seen in Figures (4-1), (4-2), (4-3), and (4-4). It is indicated good homogeneity and fine incorporation of PbO particles in the polymer films, which was improved with the increasing the proportions level. This presented a successful preparation method that forms suitable conditions and used to prepare these composite films [102].

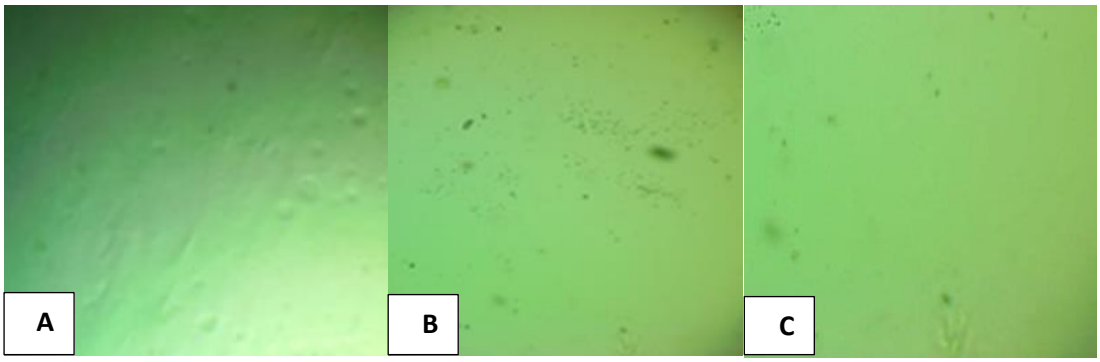

Figure (4-1): Photomicrographs (10X) for PMMA, with different thicknesses (A=60, B=120, C=220)µm.

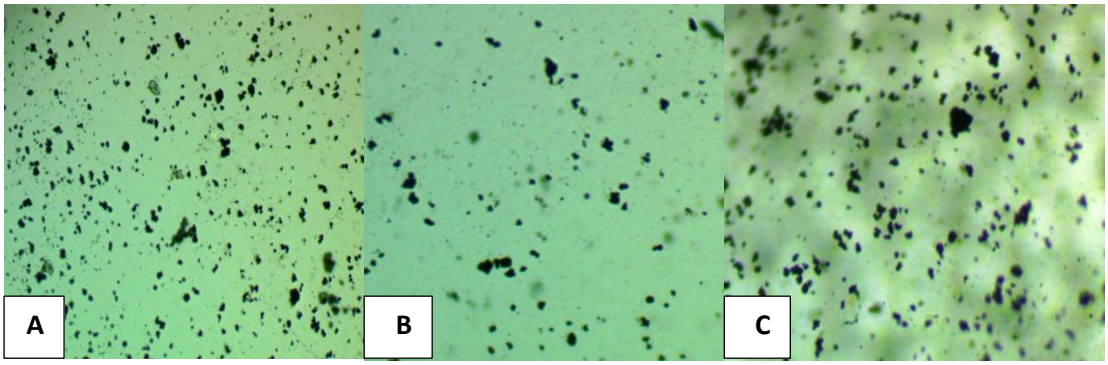

Figure (4-2): Photomicrographs (10X) for (PMMA-PbO), with different thickness(A=60, B=120, C=220)µm, at 1wt% of PbO.

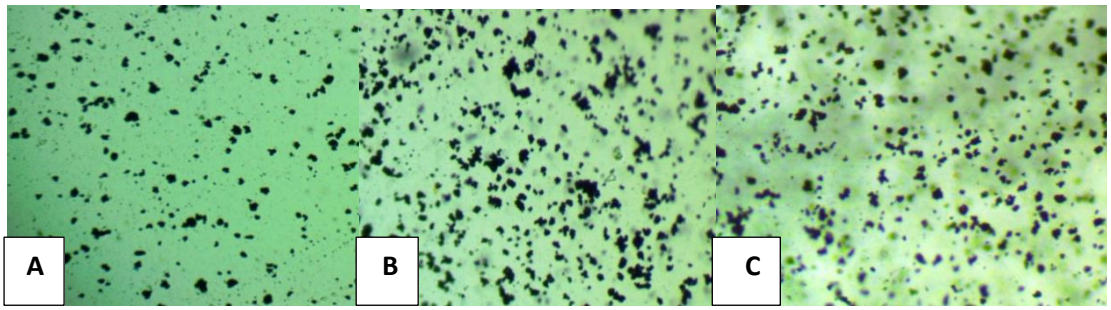

Figure (4-3): Photomicrographs (10X) for (PMMA-PbO), with different thickness(A=60, B=120, C=220)µm, at 2wt% of PbO.

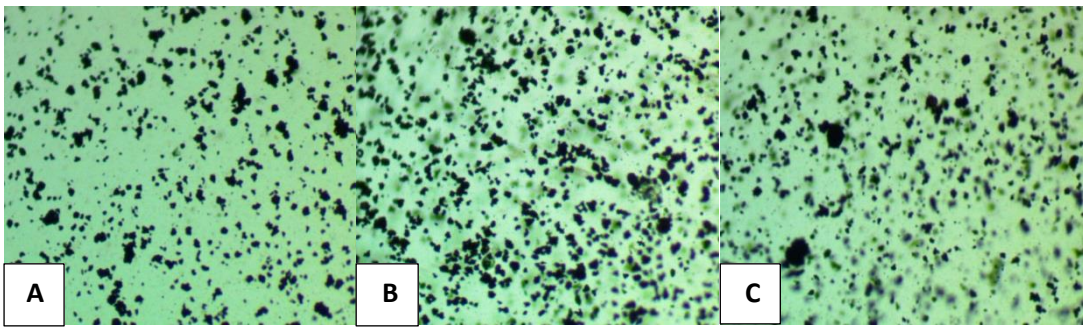

Figure (4-4): Photomicrographs (10X) for (PMMA-PbO), with different thickness(A=60, B=120, C=220)µm, at 3wt% of PbO.

4.2.2 Fourier Transform Infrared Radiation (FTIR) of(PMMA-PbO) Nanocomposites.

FTIR spectroscopy used to analyze the interactions among atoms or ions in (PMMA-PbO) nanocomposites, these interactions can include changes in the vibrational modes of the nanocomposites [103].

Figures (4.5),(4.6),(4.7), and (4.8) show the FTIR spectra of (PMMA-PbO) nanocomposites at different concentrations (0,1,2 , and 3) wt% of (PbO), and different thicknesses (60,120, and 220)μm. It has been registered in the range (4000-1000) cm^{-1}. In Figure (4.5) (A), the FT-IR range of nanocomposites is shown peak at 2950.08 cm^{-1}, this peak is recognized as stretching vibrations of (C-H), the absorption band at 1721.14 cm^{-1} is characteristic of C=O stretching vibration from PMMA. The band at 1434.92cm^{-1} attributed to C-H bending while, the absorption band at 1240.18 cm^{-1} represents C- C also from PMMA. The absorption band at 1143.79 cm^{-1} represents C-O stretching vibration in PMMA, and Figure (4.5) (B), was presented various peaks such as, 1239.78, 1143.36 cm^{-1} that were belong to CH_2 bending, (C-O) stretching, and peak at 2360.91 cm^{-1}, stretching vibrations were attributed to (O-H), the peak at 1719.71cm^{-1} C=O stretching, and FT-IR spectrums of Figure (4-5) (C), shown stretching vibrations of (C-H) at 1435.02cm^{-1}, and peak at 1720.76 cm^{-1} of (C=O), and two peaks at 1240.18, 1143.73 cm^{-1} of CH_2, C-O bonds, respectively [104]. In the case of (PMMA-PbO) with different PbO ratios , and different thicknesses, when compared to a pure PMMA film, the FT-IR spectrum reveals a shift in the location of the peaks, as well as changes in the form and intensity of the peaks and bands. Using this example, we can see how the interaction of PbO nanoparticles with the polymer results in a decoupling of the associated vibrations [105], and it was observed that when the amount of lead oxide nanoparticles increased, the transmittance decreased. The increased density of the films results in a rise in the number of atoms and ions in the light path, as well as an increase in the UV absorbance inverse the IR absorbance, as seen in Figures (4.6), (4.7), (4.8). (A-B-and C) , these findings are similar to previous study findings [106].

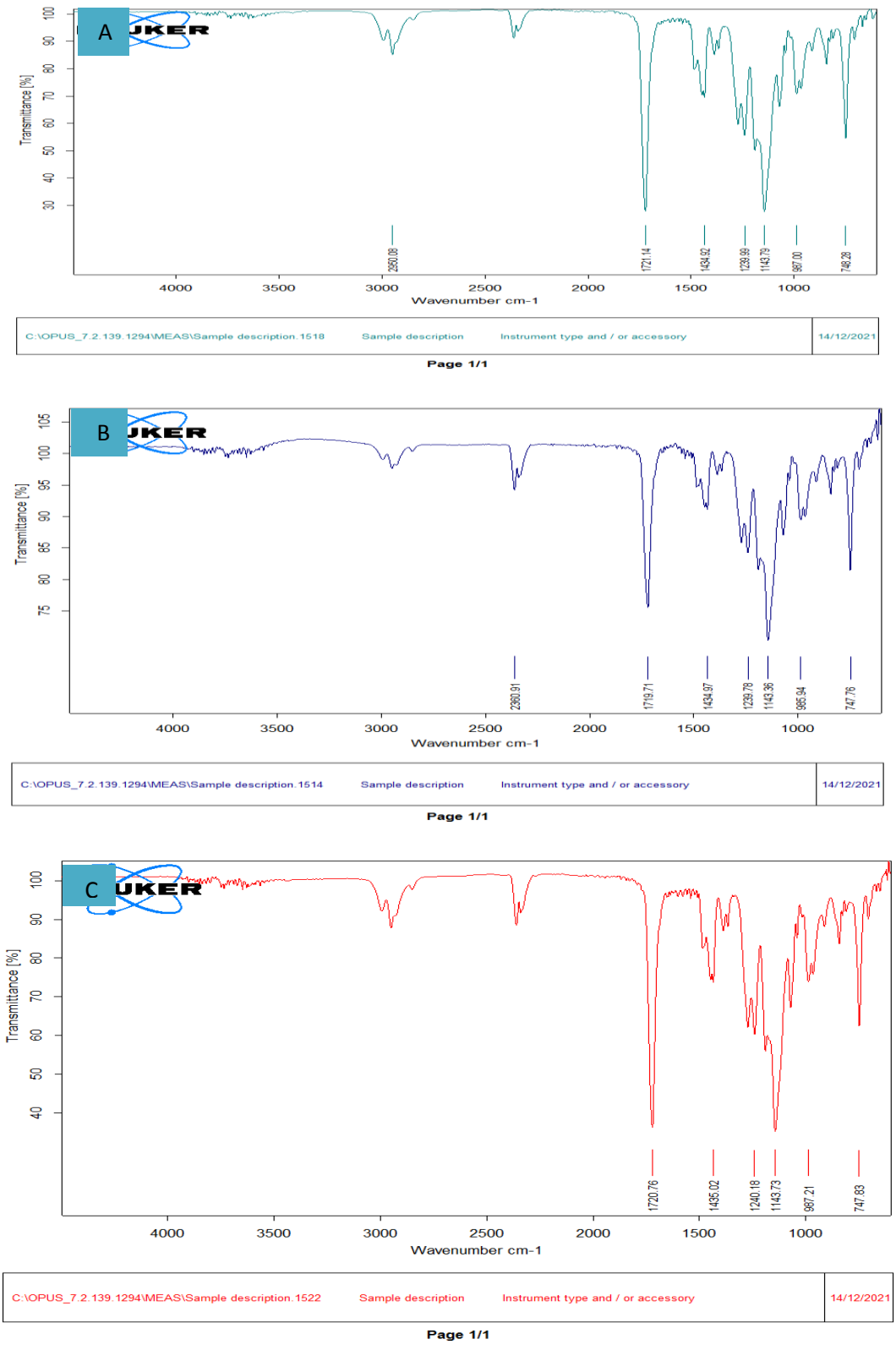

Figure(4.5): FTIR spectra of pure PMMA with different thickness (A=60, B=120, and C=220)µm.

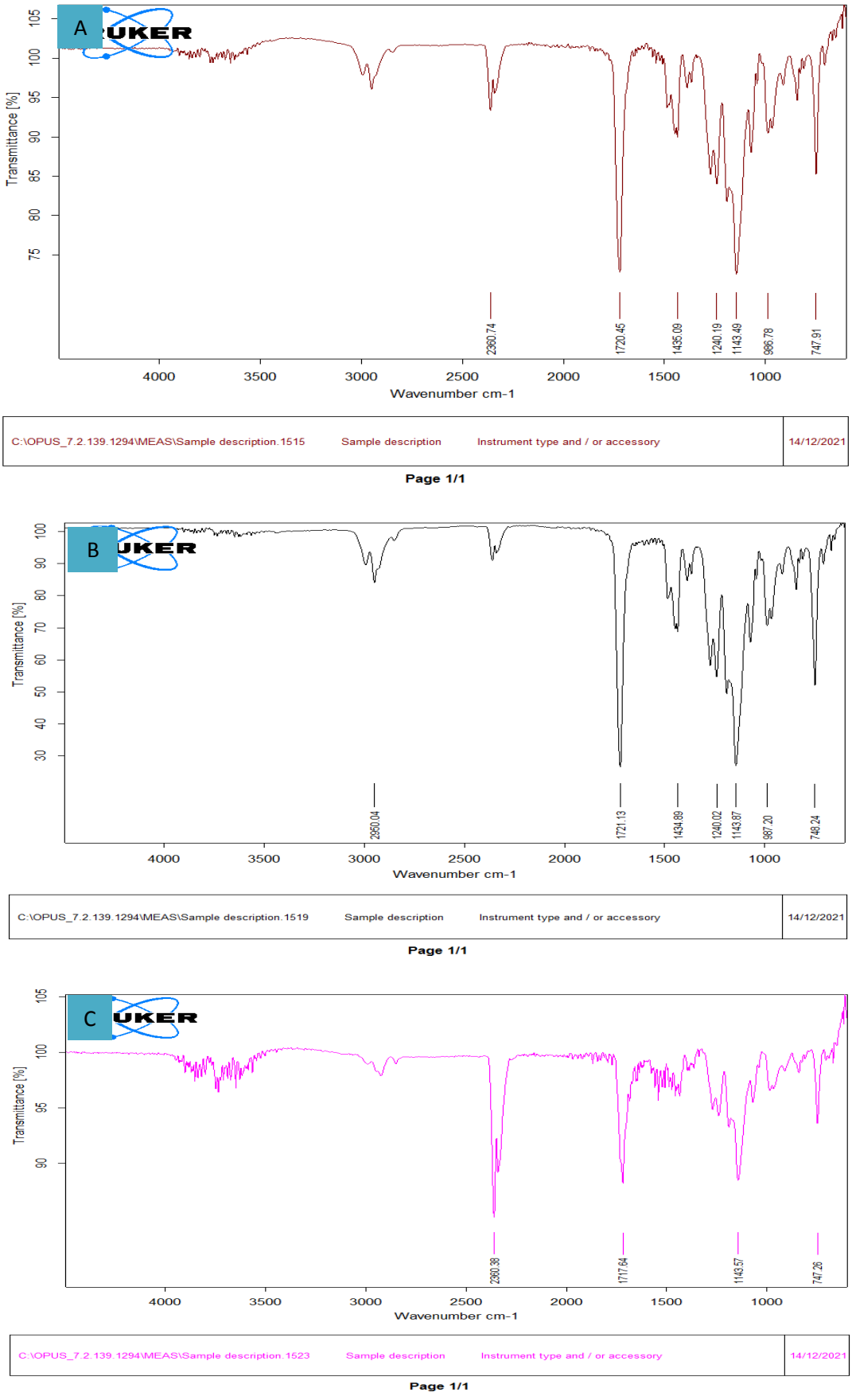

Figure (4.6): FTIR spectra of (PMMA-PbO) nanocomposites at 1wt% of PbO with different thicknesses (A=60, B=120, and C=220) µm.

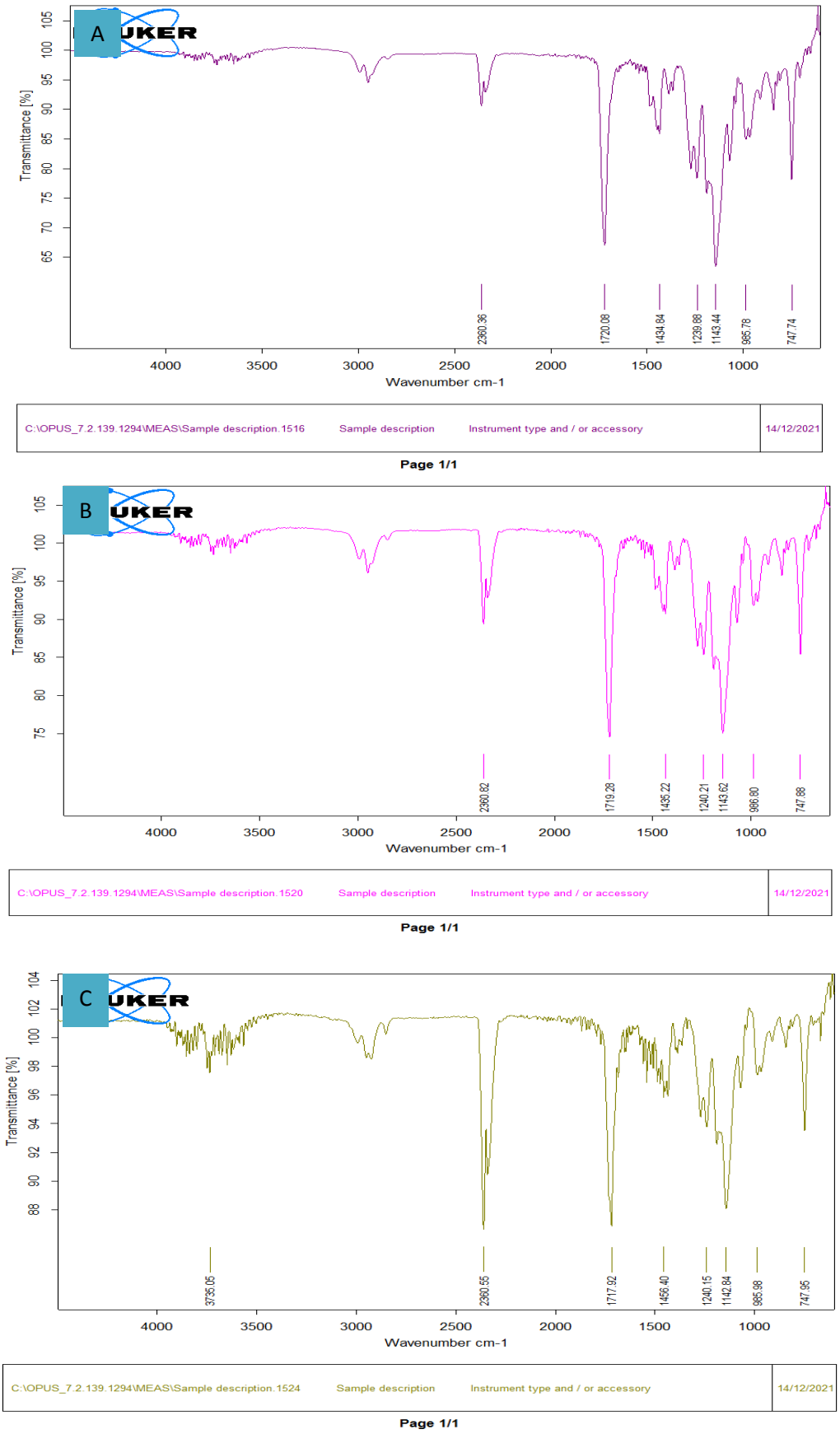

Figure (4.7): FTIR spectra of (PMMA-PbO) nanocomposites at 2wt% of PbO with different thicknesses (A=60, B=120, and C=220) µm.

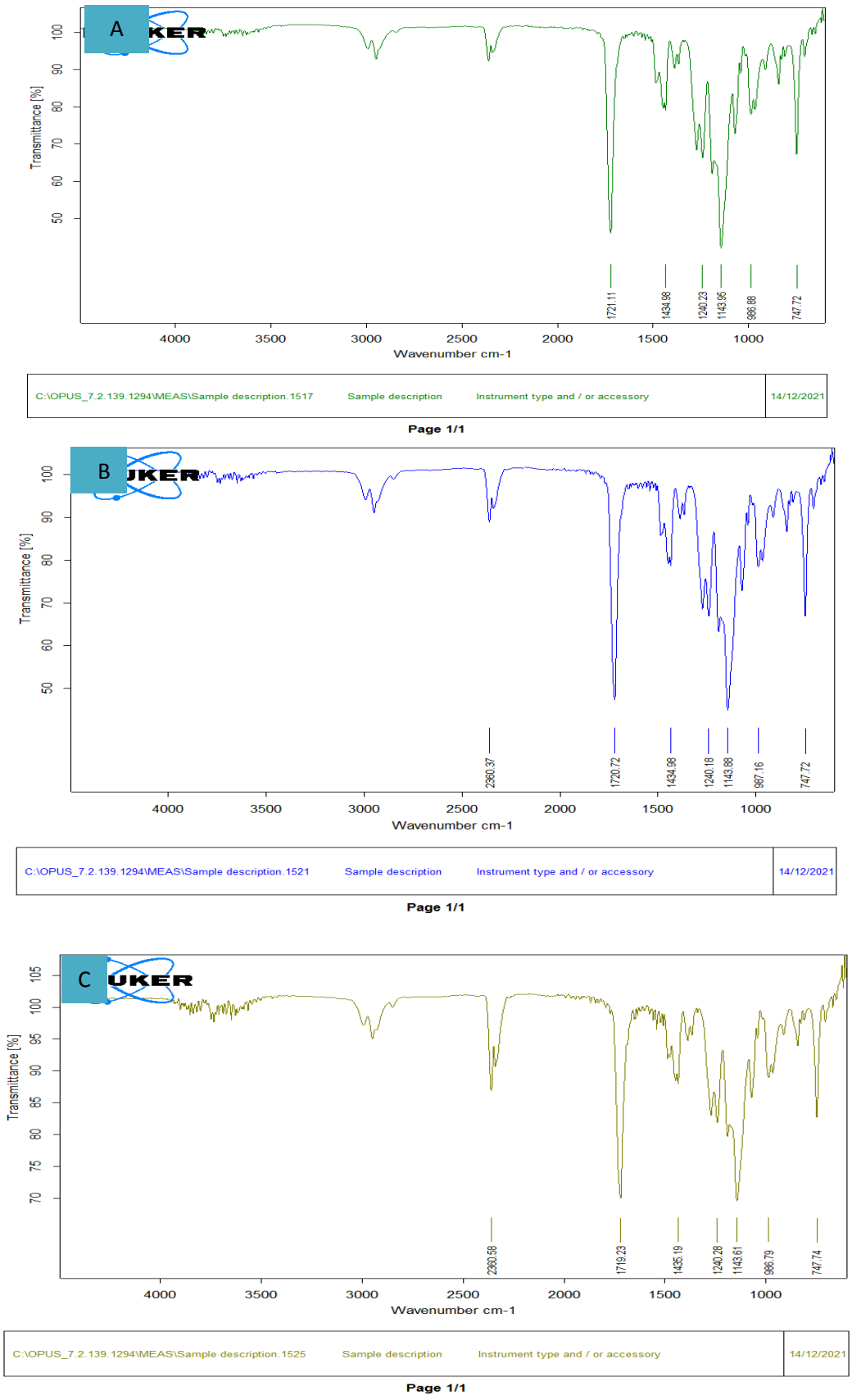

Figure (4.8): FTIR spectra of (PMMA-PbO) nanocomposites at 3wt% of PbO, with different thicknesses (A=60, B=120, and C=220) µm.

4.2.3 Scanning Electron Microscopy (SEM)

SEM technique is used to quantify the dispersion of nanocomposites particles inside the polymer matrix and to conduct a complete investigation of the influence of lead oxide nanoparticles material. SEM images of the (PMMA-PbO) nanocomposites films with various concentrations of Lead Oxide nanoparticles content are shown in Figure (4.9). Since image (A) is found in Figure (4.9), the polymer is softer, homogeneous, and cohesive, and as shown in the figures below, the inclusion of Lead Oxide nanoparticles in the compounds makes the polymer softer, homogeneous, and cohesive (PMMA- PbO). They lead to changes in surface morphology. It is clear from the picture that the grain clumps with an increase in the lead oxide nanoparticles. as seen in the picture. The findings would demonstrate the membranes' surface morphology (PMMA-PbO).The number of aggregates or fragments randomly distributed on the upper surface of nanoparticles increases as the concentration of lead oxide nanoparticles increases [107,108].

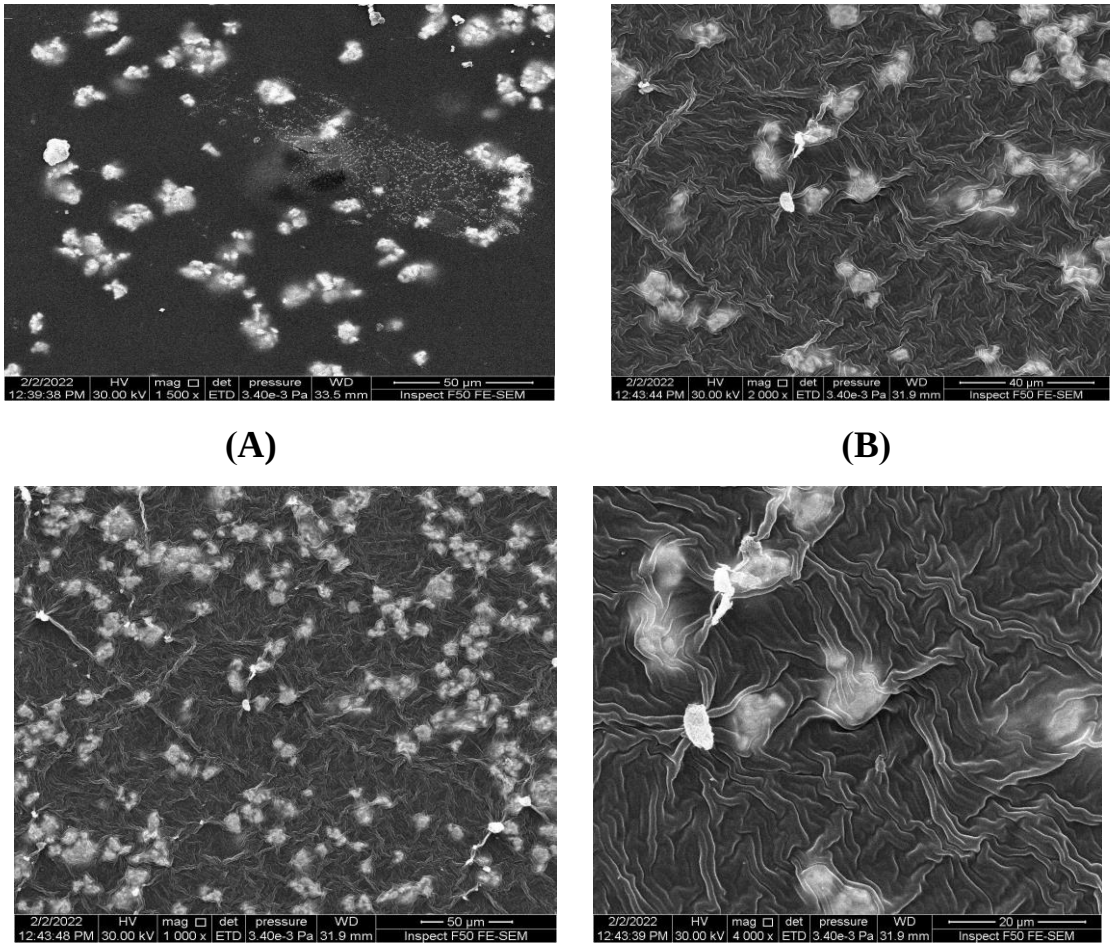

Figure (4.9): FE-SEM images for (PMMA-PbO) nanocomposites (A) for pure PMMA (B) for 1wt.% PbO , (C) for 2wt.% PbO , (D) for 3wt.% PbO.

4.3 The Optical Properties

4.3.1 Absorbance (A).

The absorbance of (PMMA-PbO) nanocomposites was recorded for different thickness films for a range of wavelengths (180-1100) nm at room temperatures. Figure (4.10) shows the difference in absorbance of the nanocomposites (PMMA-PbO) with the wavelengths of the incident light. Therefore, it gets high absorbance of samples for nanocomposites in the UV zone due to photon energy enough to interact with the atoms. By absorbing the photon with known energy variations, the electron is excited from a lower to a higher level of energy. Variations in the

absorbed and transmitted radiation can determine the types of possible electron transitions. Fundamental absorption of the absorbance spectra refers to the band or to the transition of the excitation [109]. In near-infrared and visible regions, the absorption of all specimens for nanocomposites has a low value, and this behavior is caused by the energy of the incident photons; there is insufficient energy to interact with the atoms, so photons will be emitted as the wavelength increases. The figure showed that increasing the film thickness increased the absorbance, this is because incoming light is absorbed by free electrons [110]. Additionally, increasing the weight proportions of lead oxide nanoparticles results in an increase in absorbance [111]. As shown in the figure, the absorbance has a higher value at 3wt% of PbO nanoparticles.

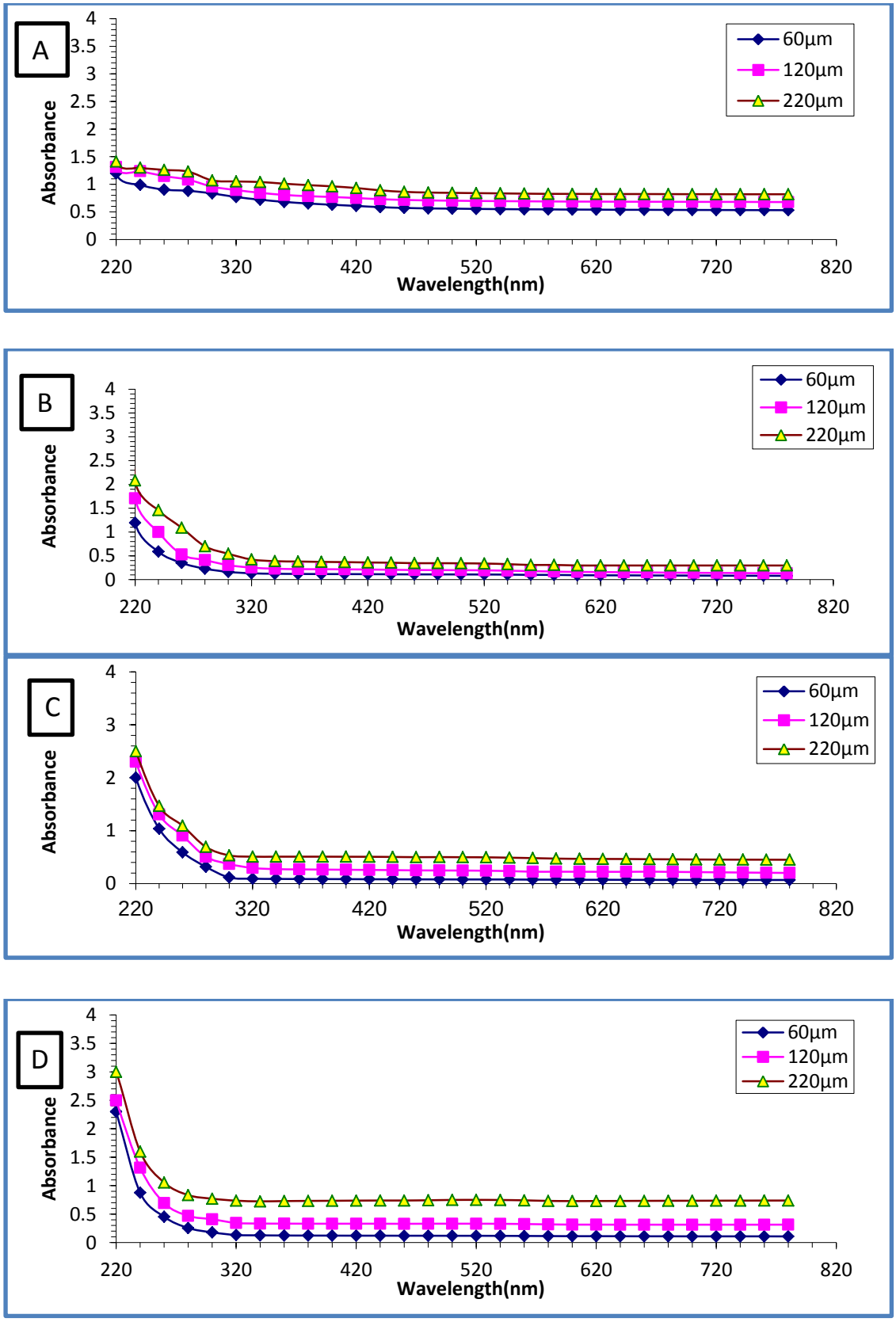

Figure (4.10): The absorbance variation of (PMMA-PbO) nanocomposites as a function of wavelength at different thicknesses.With different loading (A=0, B=1, C=2, and D=3) wt% of PbO nanoparticles.

4.3.2 The transmittance of (PMMA-PbO) Nanocomposite.

Figure (4.11) shows the optical transmittance spectrum as a function of the wavelength of incident light on (PMMA-PbO) films of different thicknesses and at different concentrations (0,1,2, and 3) wt% of lead oxide. The figure showed that the transmittance increases gradually according to the increase in wavelength and for all films due to a decrease in the absorbance with the wavelength, while the transmittance decreases with increasing thickness, the reason for the decrease in transmittance with increasing thickness is that it depends largely on the thickness factor. The reason for this is that the large thickness leads to the occurrence of the phenomenon of optical absorption, thus attenuating a large part of the radiation falling on the film [112]. Additionally, the figure illustrates the transmittance decrease with the increased concentration of (PbO) nanoparticles, this is caused by added (PbO) nanoparticles contain electrons in it are outer orbits can absorb the electromagnetic energy of the incident light and travel to higher energy levels, this process is not accompanied by the emission of radiation because the traveled electron to higher levels has occupied vacant positions of energy bands, thus part of the incident light is absorbed by the substance and does not penetrate through it [113].

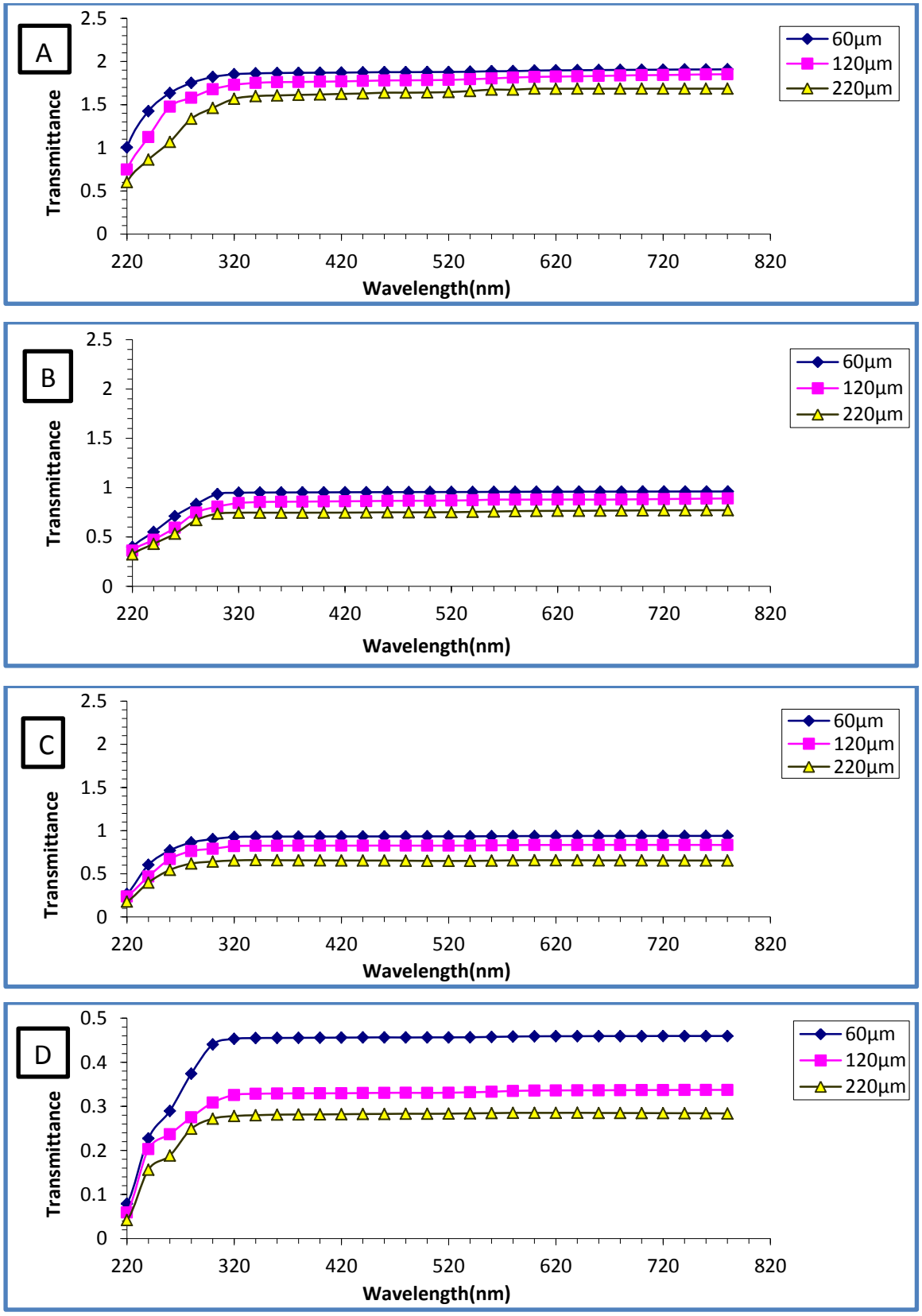

Figure (4.11): Transmittance spectra (PMMA-PbO) Nanocomposites as a function of wavelength at different thicknesses, with different loading (A=0, B=1, C=2, and D=3) wt% of PbO nanoparticles.

4.3.3 Absorption Coefficient (α).

The absorption coefficient(α) is calculated by using Equation (2.5) Figure (4.12) shows the absorption coefficient (α) as a function of photon energy for (PMMA-PbO) nanocomposites. It can be seen that the absorption coefficient is the smallest at high wavelength and low energy, this means that the possibility of electron transition is little because the energy of the incident photon is not sufficient to move the electron from the valence band to the conductive band ($hv < E_g^{opt}$) [114]. At high energies absorption is bigger, this indicates that there is a high likelihood of electron transitions. As a result, the incident photon's energy is sufficient to transfer the electron from the valence band to the conduction band, indicating that the incident photon's energy exceeds the forbidden energy difference. This demonstrates how the absorption coefficient can help determine the nature of an electron transfer, when the values of the absorption coefficient are high ($\alpha > 10^4$) cm^{-1} at high energies it is expected that direct transition of an electron occurs, the energy and moment are maintained by the electrons and photons, on the other hand, because the values of the absorption coefficient are low ($\alpha < 10^4$)cm^{-1} at low energies, it is expected that indirect transition of an electron occurs, and the electronic momentum is maintained with the assistance of the phonon [115], among other results is that the coefficient of absorption for the (PMMA-PbO) nanocomposites is less than (10^4 cm^{-1}), this explain that the electron transition is indirect. The figure shows that the absorption coefficient of the (PMMA-PbO) has a higher value at 3wt.% of PbO nanoparticles.

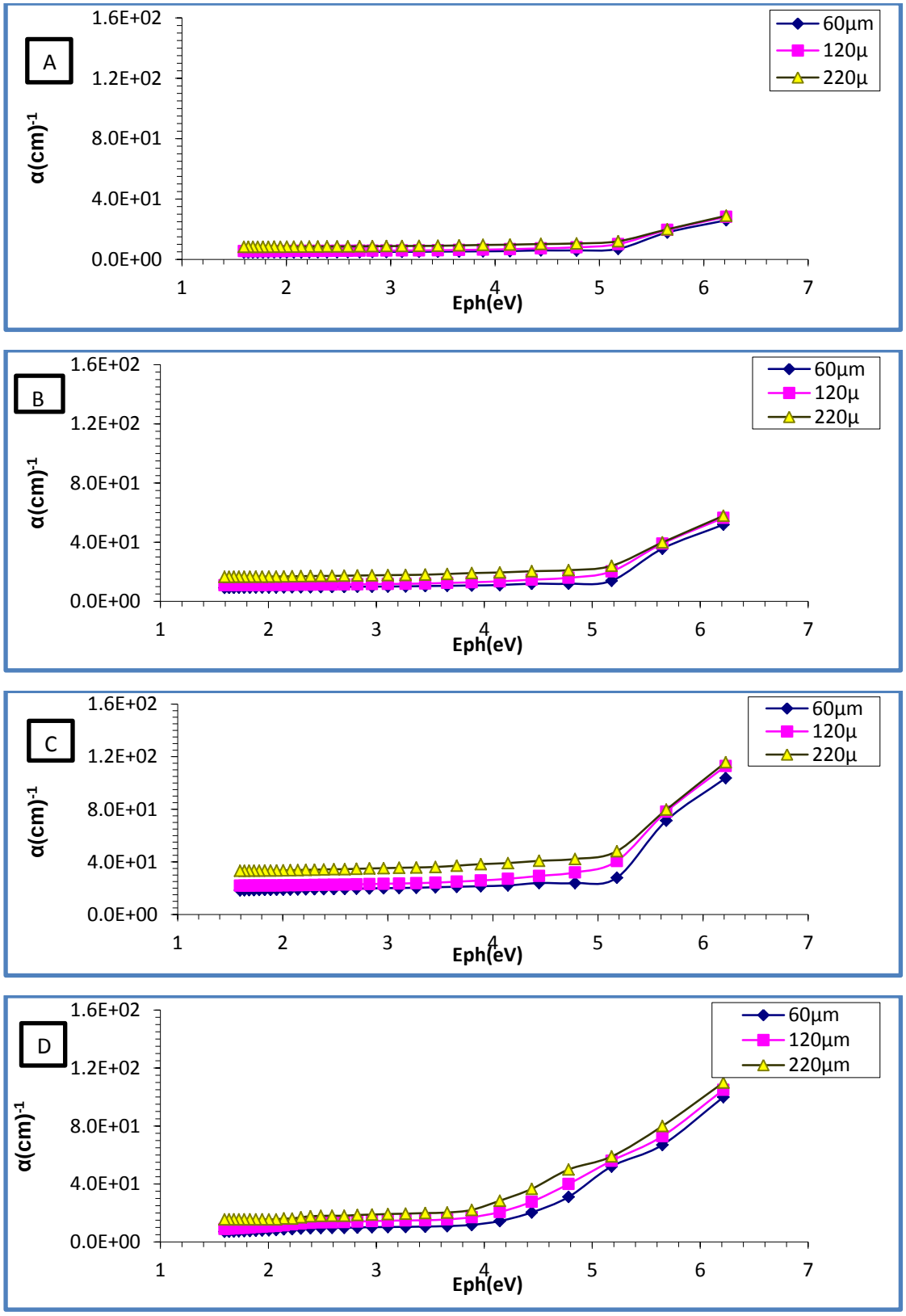

Figure (4.12): The absorption coefficient variation of (PMMA-PO) nanocomposites with the photon energies. With different loading (A=0, B=1, C=2, D=3) wt% of PbO nanoparticles.

4.3.4 Energy gaps of the (allowed and forbidden) indirect transition

Both the permitted and prohibited indirect transition band energy gap is determined using Equation (2.7). When the value of r =2 the permitted indirect transition band energy gap is calculated, but when the value of r =3 the prohibited indirect transition band energy gap is calculated. Figure (4.13) clarifies the energy gap for the allowed indirect transition $(\alpha h\upsilon)^{1/2}$ $(cm^{-1}.eV)^{1/2}$ versus photon energy of (PMMA-PbO) nanocomposites, to calculate the energy gap, drawing a straight line from the upper part of the curve in Figure (4.13) to the (x) axis for the allowed indirect transition [116]. Figure (4.13) demonstrated a reduction in the energy gap as the thickness of the films increased, and this energy gap reduction might be a result of the presence of unstructured defects, which increase the density of localized states in the energy gap, hence decreasing the energy gap [117]. It is obvious that as the proportions of lead oxide nanoparticles increase the energy gap's values decrease. This is due to site levels are being created inside the restricted energy gap. Because of the increase in the ratio of lead oxide nanoparticles, a transition occurs in which electron transfers from the valence band to the local conduction belt, which explains the reduction in the energy gap with the increase in lead oxide nanoparticles [118]. Similarly, the prohibited transition of the indirect energy gap is determined. Figure (4.14) shows the prohibited transition of the (PMMA-PbO) nanocomposites' indirect energy gap. The value in Table (4.1) indicates that the (PMMA-PbO) nanocomposites have a lower value for energy gap at 3wt% of PbO nanoparticles the more we get a lower energy gap, the better the work will be and the closer we get to the semiconductor.

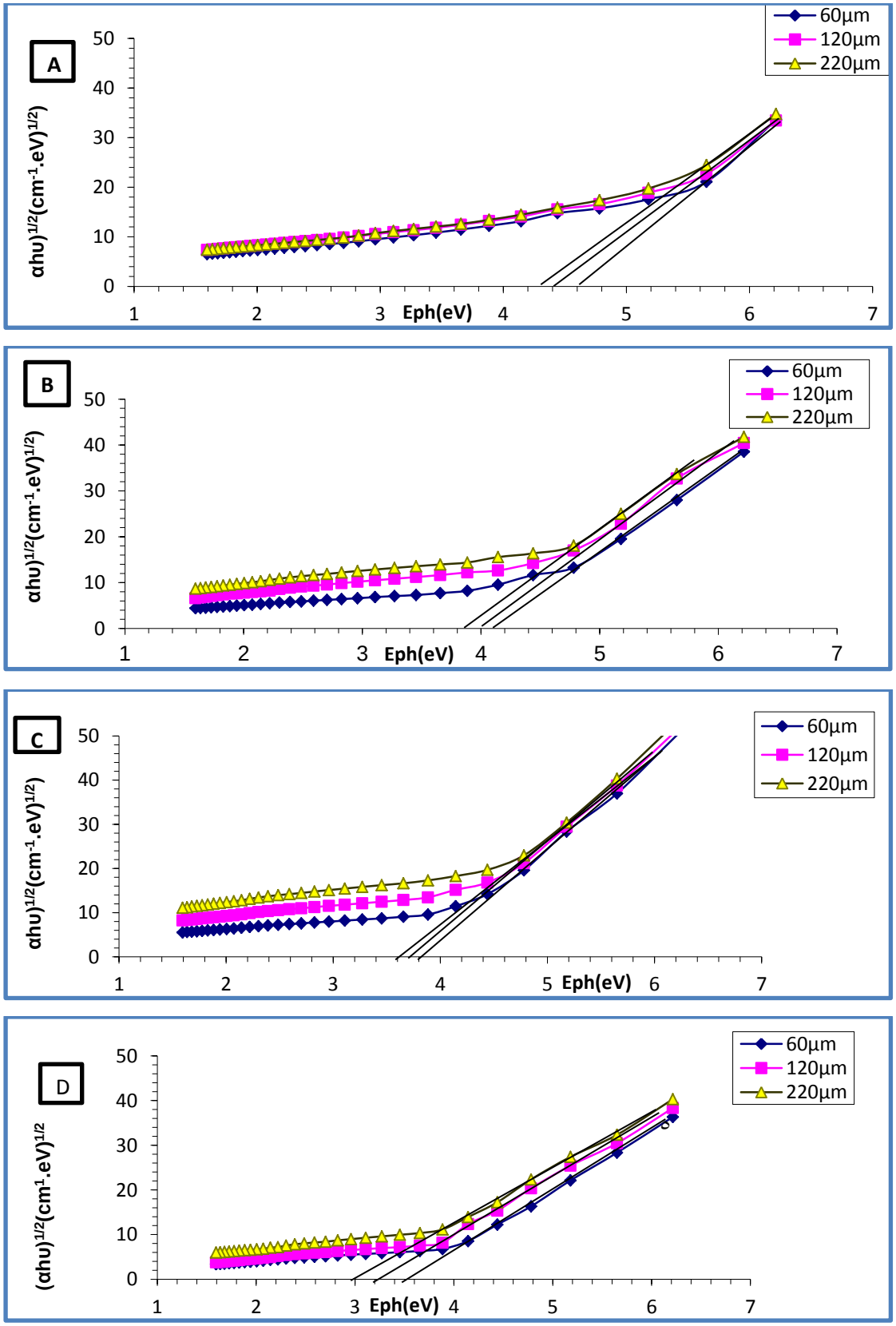

Figure (4.13): The energy gap for the allowed indirect transition $(\alpha h\upsilon)^{1/2}$ $(cm^{-1}.eV)^{1/2}$ versus photon energy of E_{ph}(ev) (PMMA-PbO) nano-composite with different thickness. With different loading (A=0, B=1, C=2, D=3) wt%of PbO nanoparticle.

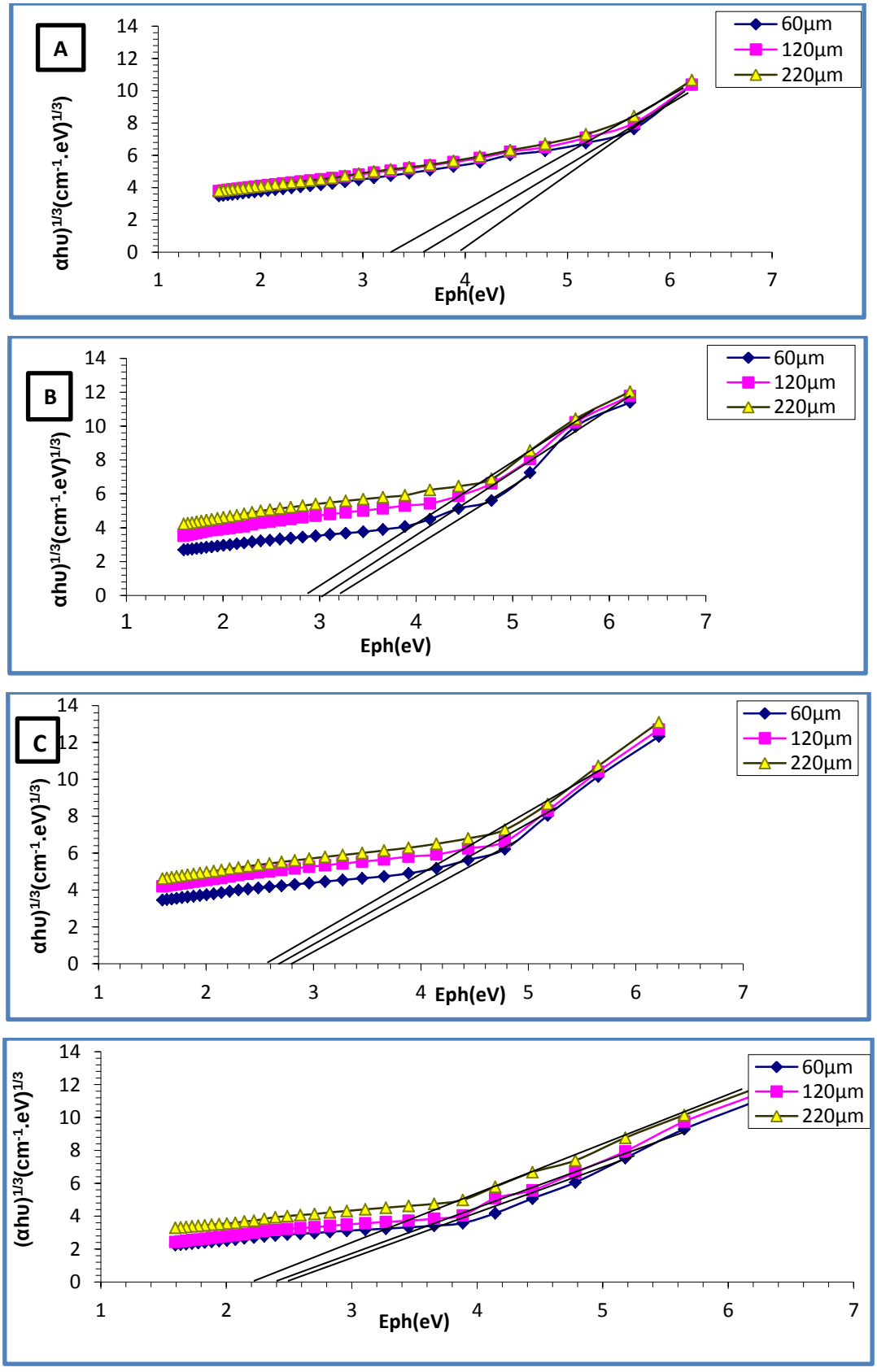

Figure (4.14): The Energy gap for the forbidden indirect transition (α hυ) $^{1/3}$ (cm$^{-1.}$ eV) $^{1/3}$versus photon energy E_{ph}(ev) of (PMMA-PbO) nano-composite with different loading (A=0, B=1, C=2, and D=3) wt% of PbO nanoparticles.

Table (4.1): Energy Gap Values for Allowed and Prohibited Indirect Transitions in (PMMA-PbO) Nanocomposites.

Thickness (μm)	(PbO)wt% Nanoparticles concentration	Permitted Indirect Transition (ev)	Prohibited Indirect Transition(ev)
60	0	4.6	4
120		4.4	3.6
220		4.3	3.3
60	1	4.1	3.2
120		4	3
220		3.9	2.9
60	2	3.8	2.8
120		3.7	2.7
220		3.6	2.6
60	3	3.5	2.5
120		3.2	2.4
220		3	2.2

4.3.5 Refractive Index (n)

The refractive index was determined using the values of reflection (R) in Equation (2.10). Figure (4.15) shows the relationship between wavelength for nanocomposites (PMMA-PbO) and refractive index. From the figures the increase in the thickness of the film led to an increase in the refractive index, and, this behavior may be due to improvement in the structure of the film, reduction of dangling bonds and defects like vacancy sites, it yields more packing density [119], and the figure also shows that the refractive index increases with the increase in the concentration of nanoparticles (PbO) due to the increase in the density of nanocomposites in the UV region, and in visible and near IR region, low values are noted due to high transmittance [120]. The Figure (4.15)

showed that the refractive index has a higher values at 3wt% of PbO nanoparticles.

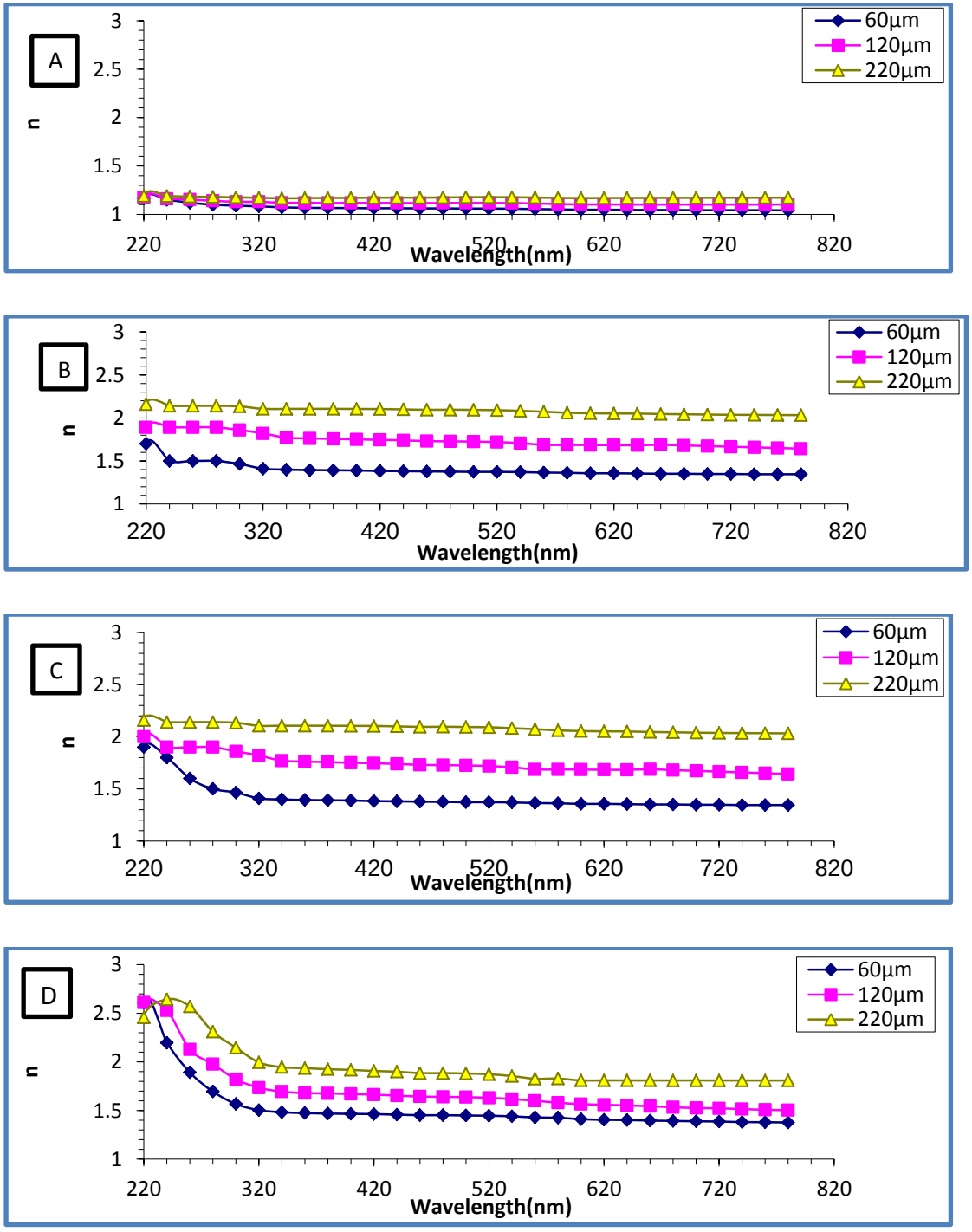

Fig (4.15): Relationship between refractive index(n) for (PMMA-PbO) nano-composites with the wavelengths(nm), at different thicknesses with different loading (A=0, B=1, C=2, D=3) wt% of PbO nanoparticles.

4.3.6 Extinction Coefficient (K_0)

Extinction coefficient (k) can be calculated by using Equation (2.11). Figure (4.16) illustrates the variation in the extinction coefficient with wavelength for (PMMA -PbO) nanocomposites. The figure indicates that as the thickness of the film increases, so does the extinction coefficient, the reason for this increase is attributed to the fact that the increase in thickness led to an increase in the number of photon collisions with the material, and thus the absorbance of the material will increase, and then the extinction coefficient will increase [35]. Also, it can be noted that the extinction coefficient increases with the increase of (PbO) nanoparticles. This is attributed to the increased absorption coefficient with the increase of weight percentages of Lead oxide nanoparticles. This result indicates that the atoms of (PbO) nanoparticles will modify the structure of the host polymer [34]. Figure (4.16) noted that the extinction coefficient has a higher values at 3wt% of PbO nanoparticles.

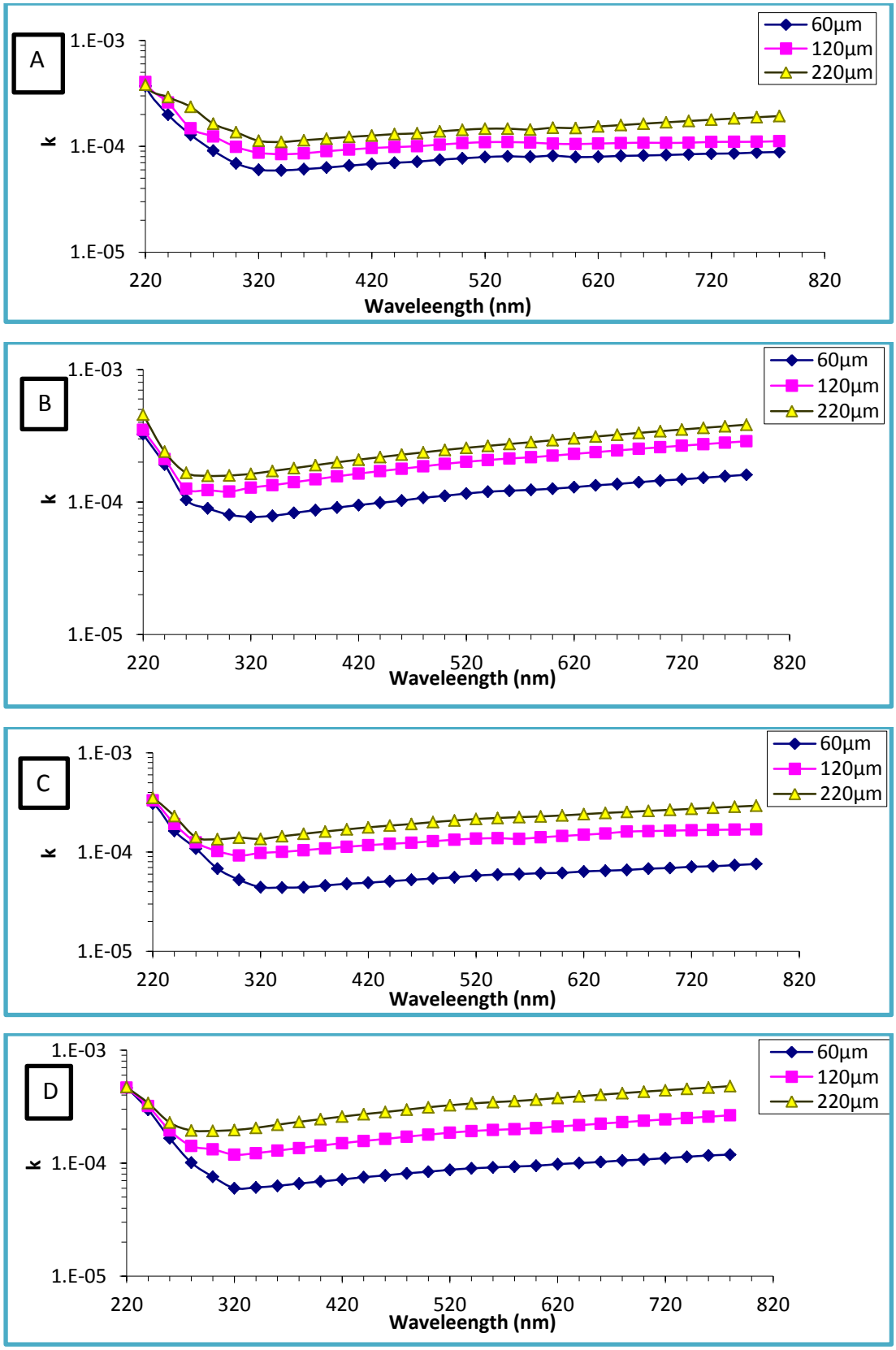

Fig (4.16): The relationship between the extinction coefficient and wavelength for different thickness (PMMA-PbO) nanocomposites, with different loading (A=0, B=1, C=2, and D=3) wt% of PbO nanoparticles.

4.3.7 The Real and Imaginary Parts of Dielectric Constant (ε_1, and ε_2).

The real and imaginary parts of dielectric constants (ε_1, and ε_2) can be represented as shown in Figures (4.17), and (4.18) for films (PMMA-PbO) nanocomposites. From these figures, it is noticed that the behavior of ε_1 was the same as the refractive index due to the small values of k^2 compared to n^2, whereas ε_2 basically relies on the values of k, that is connected to the variety of absorption coefficient. Also, it is seen that the maximum values of the ε_1 and ε_2 were reached in the low wavelength region (absorption region) and the values of ε_1 are higher than that of ε_2. The real and imaginary dielectric constants (ε_1, ε_2) for (PMMA-PbO) nanocomposites have been calculated from Equations (2.12) and (2.13), respectively [121,122].

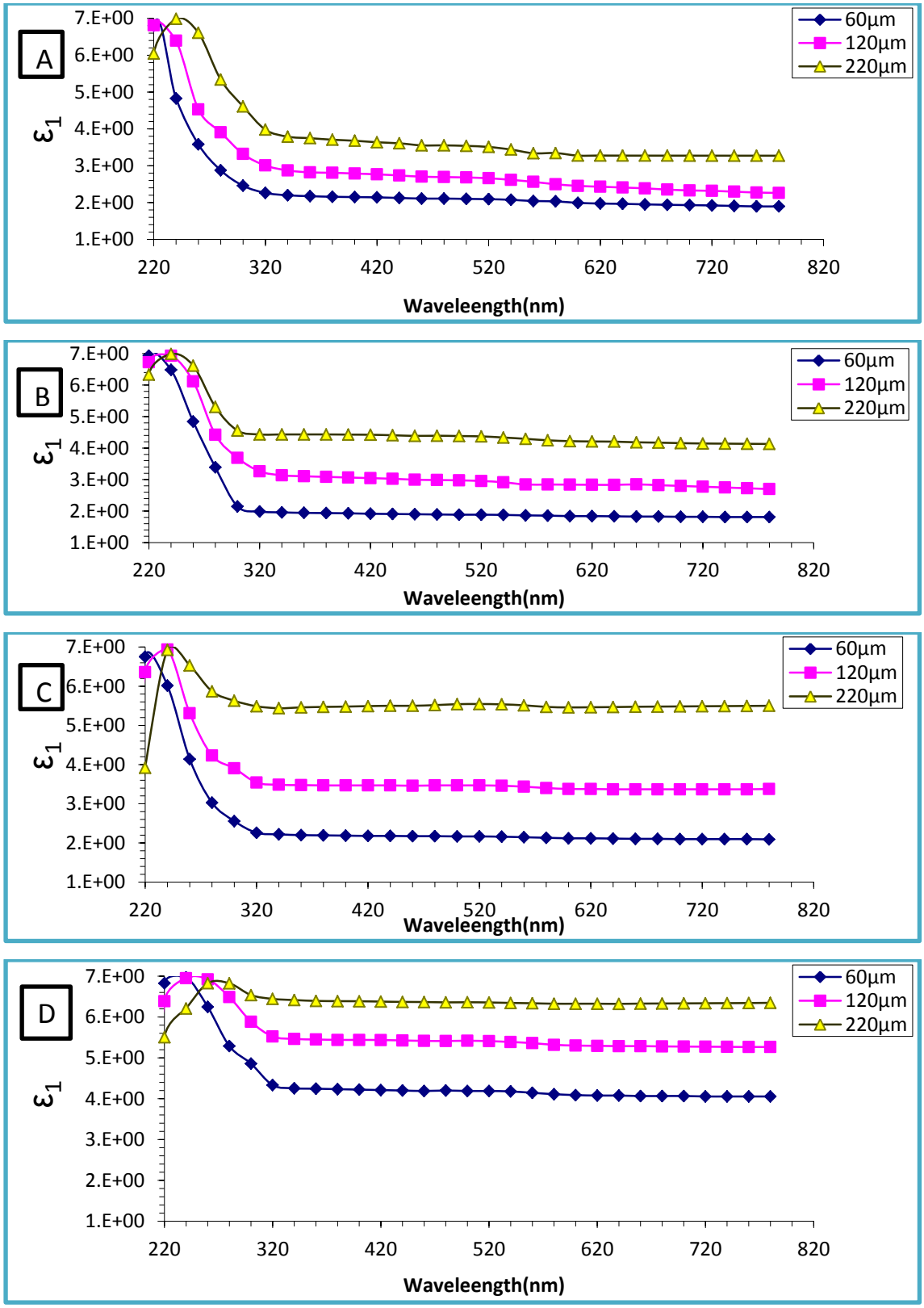

Fig (4.17): The real part ε_1 of the dielectric constant of (PMMA-PbO) nanocomposites versus with wavelength (nm), at different thicknesses, with different loading (A=0, B=1, C=2, D=3) wt% of PbO nanoparticles.

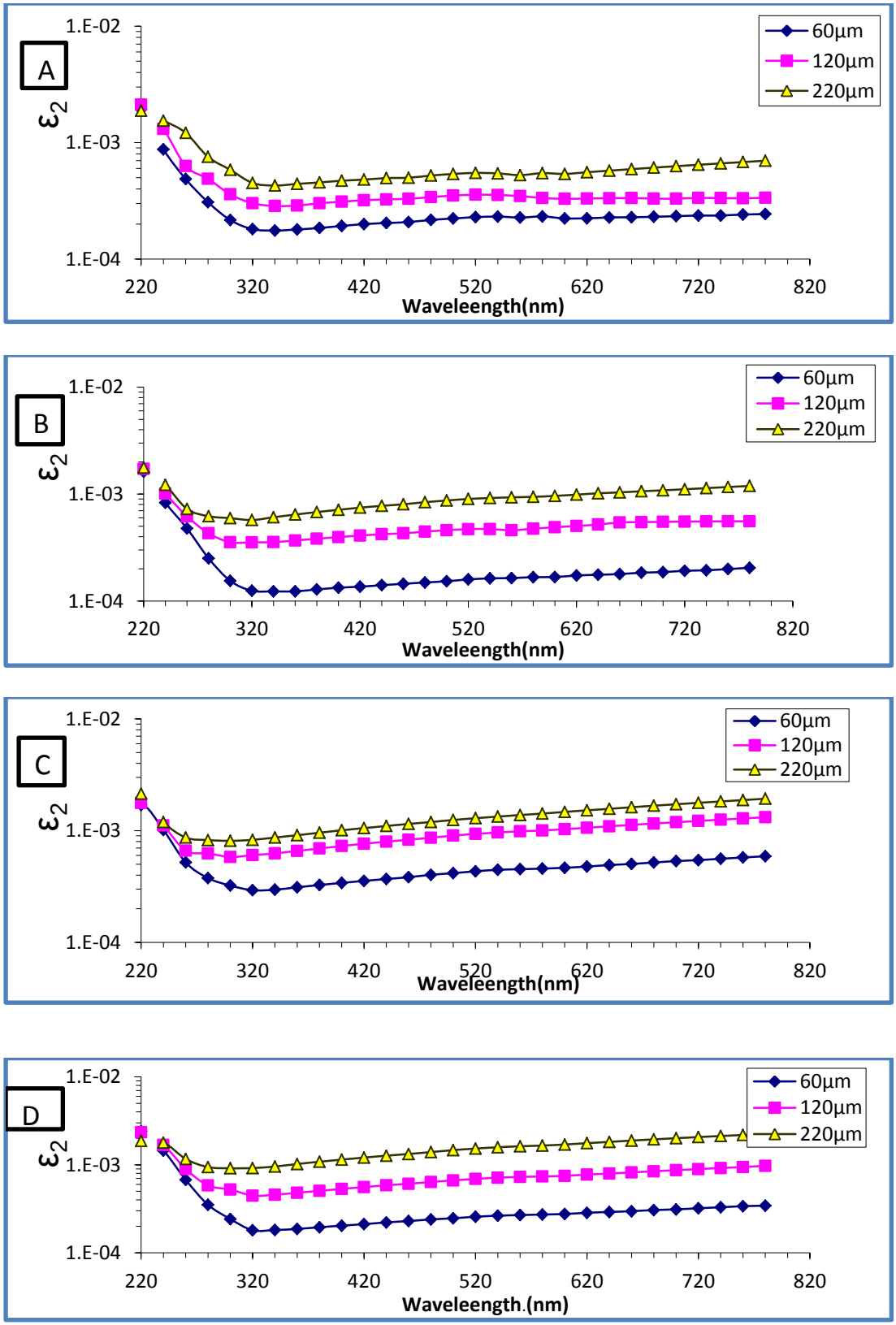

Fig (4.18): **Imaginary dielectric constant as a function of wavelength for (PMMA-PbO) nanocomposites with different thicknesses, and (A=0, B=1, C=2, D=3) wt% of PbO nanoparticles.**

4.4 The A.C Electrical Properties.

The A.C electrical properties of (PMMA-PbO) nano-composites include (dielectric constant, dielectric loss, and A.C electrical conductivity) with a frequency range (100Hz-6MHz) at room temperature.

4.4.1 The Dielectric Constant.

Figures (4.19) and (4.20) illustrate the influence of film thickness on the dielectric constant. The figures show that the dielectric constant increase with increasing the film thickness. As seen in the figures, the dielectric constant increase with the increase of the concentration of lead oxide nanoparticles. This is attributed to the formation of a continuous network of lead oxide nanoparticles inside the nanocomposite. This was well shown in the microscopic photos taken for samples of (PMMA-PbO) nanocomposites. At a low concentration of 1wt.% of the lead oxide nanoparticles take the form of clusters or separated groups; hence, the dielectric constant becomes approximately low. On the other hand, at high concentrations (3wt.%), lead oxide nanoparticles form a continuous network inside the nanocomposite and so the value of the dielectric constant increase with the volumetric rate of the lead oxide nanoparticles [123]. It is apparent from the figures that the dielectric constant decreases with increasing applied frequency, due to the forms of polarization (ionic and electronic, dipolar, space charge), at low frequencies, the polarization of the space charge plays a significant role in increasing the dielectric constant. Becomes less contributing to the rise in frequency and more contributing of polarization, and this action induces the decrease in the dielectric constant values for all samples with an increase in the frequency of the electrical field, the other types of polarizations occur at subsequent frequencies. This is because the mass of the ion is greater than

that of the electron, as a result of which the electrons respond to even the high frequency of the field vibrations, which makes the electronic polarization the only type of polarization at higher frequencies [124].

However; dipoles will barely be able to orient themselves in the direction of the applied field in the high-frequency range, hence the value of the dielectric constant is almost constant. Figures (4.19), and (4.20) show that the dielectric constant has a higher value at 3wt% of PbO nanoparticles.

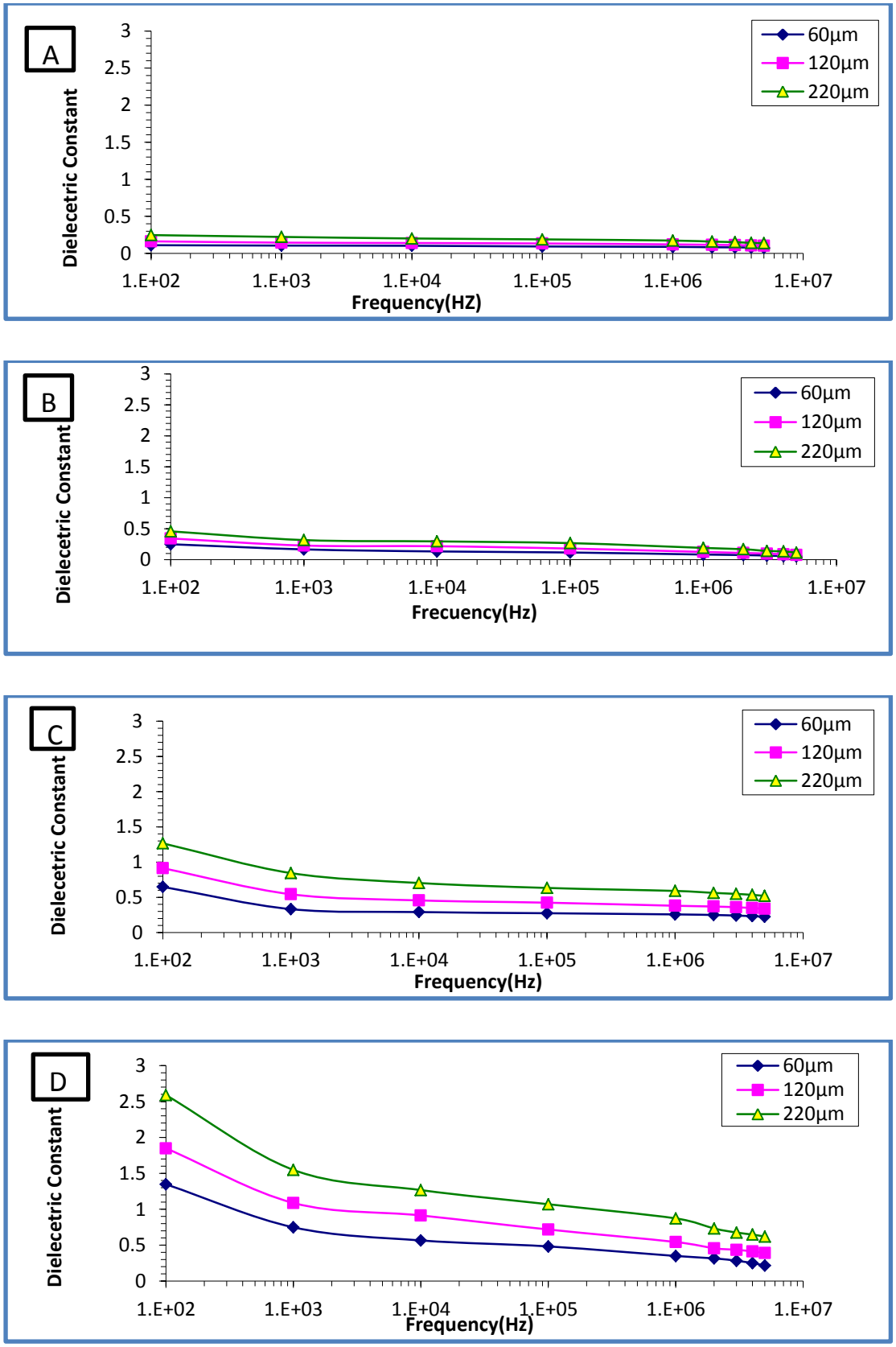

Figure (4.19): Variation of dielectric constant (ε') for (PMMA-PbO) nanocomposites with the frequency, at different thicknessesm, with different loading (A=0, B=1, C=2, and D=3) wt% of PbO nanoparticles.

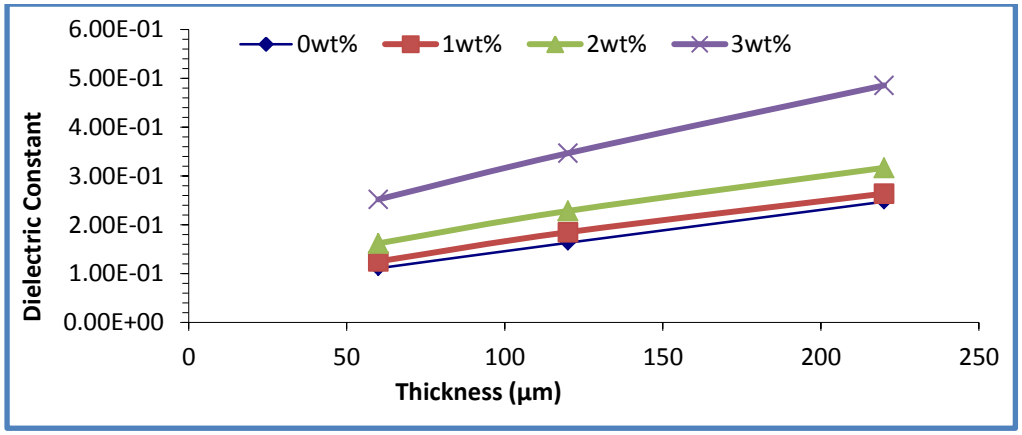

Figure (4.20): Variation of dielectric constant (ε') with the thickness of film (PMMA-PbO) nanocomposites.

4.4.2 The Dielectric Loss.

Figure (4.21) shows the dielectric loss of nanocomposites as a function of frequency. It is obvious from the figure that the values of dielectric loss are high at low applied frequency but they decrease with increasing frequency. This attributed to the decrease of the space charge polarization contribution when increasing the frequency. The highest value of the dielectric loss at f=100Hz for (PMMA-PbO) nanocomposites, this value represents the highest dielectric loss at a certain frequency, that is the highest absorption of an applied field [125]. The absorption happens due to the Maxwell-Wagner phenomenon which is caused by A.C current due to the difference of dielectric constant and conductivity of the phases in the nanocomposites. When the frequency is increasing to 2MHz, the dielectric loss is approximately constant for (PMMA-PbO) nanocomposites. This is attributed to the mechanism of other types of polarization that occurs at high frequencies [126]. By increasing the thickness of the film, the dielectric loss increases. Additionally, the dielectric loss value increases as the concentration of (PbO) nanoparticles rises due to the increase in charge carriers created by the rising PbO nanoparticle concentration, as shown in Figure (4.22).

Figures (4.21) and (4.22) show that the dielectric loss has higher value at 3wt% of PbO nanoparticles.

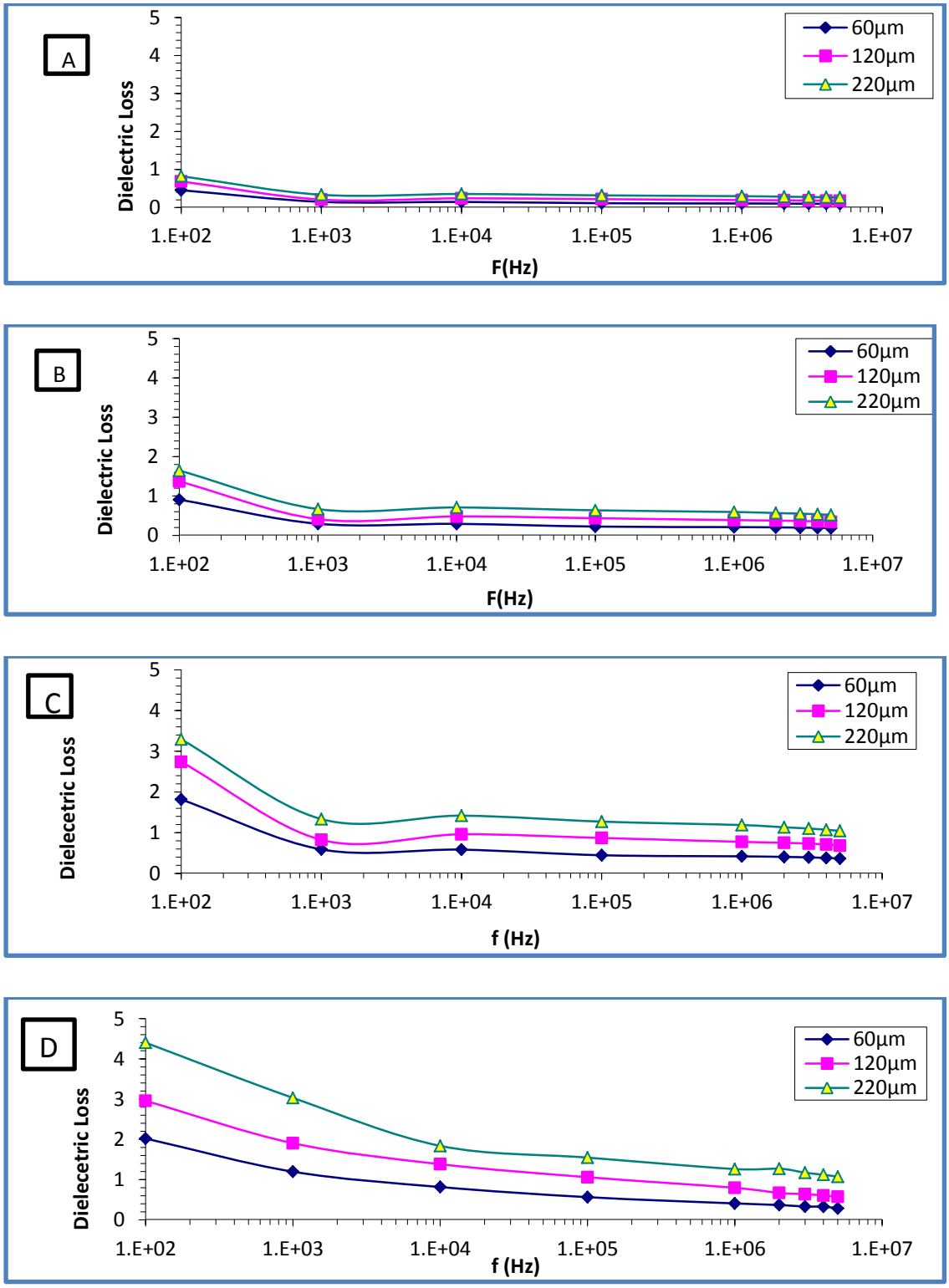

Figure (4.21): Dielectric loss (ε") variation with the frequency for (PMMA-PbO) nanocomposites, at different thicknesses. With different loading (A=0, B=1, C=2, D=3) wt% of PbO nanoparticles.

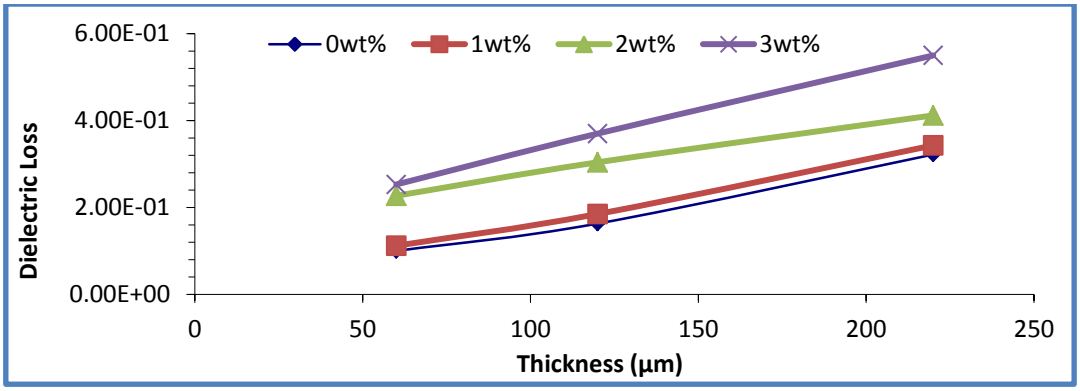

Figure (4.22): Dielectric loss (ε") variation with the thickness of the films for (PMMA-PbO) nanocomposites.

4.4.3 The A.C electrical conductivity

The variation of A.C electrical conductivity as a function of frequency for (PMMA-PbO) nanocomposites at 100Hz, is depicted in Figure (4.23). The figure demonstrates that the electrical conductivity of nanocomposites increases with increasing the frequency in (low, moderate, and higher) frequency regions this is due to the hop-up of charge carriers in the localized state and also to the excitation of charge carriers in the conduction band in the upper regions. Two influences that affect A.C conductivity are main chain motion and ion motion, in other words, the increasing in A.C electrical conductivity at low-frequency areas can be related to interfacial polarization while the increase in conductivity is due to the passage of electrons at frequencies, intermediate and the high [127]. Figure (4.24) showed that the conductivity of nanocomposites increased with increasing the film thickness, the increase in the conductivity upon increasing thickness can be attributed to the increased number of carriers available for transport due to improvement in the structure of the film with the increasing of thickness, yields more packing density reducing dangling bonds, the trapping centers of charge carriers, and defects like vacancy sites [119]. Additionally, as seen in Figure (4.24), when the proportion of (PbO)

nanoparticles increase the conductivity of nanocomposites rises, as a consequence of a rises in ionic charge carriers and the formation of an internal network of (PbO) nanoparticles at the composites [128]. Figures (4.23) and (4.24) show that the conductivity has a higher value at 3wt% of PbO nanoparticles.

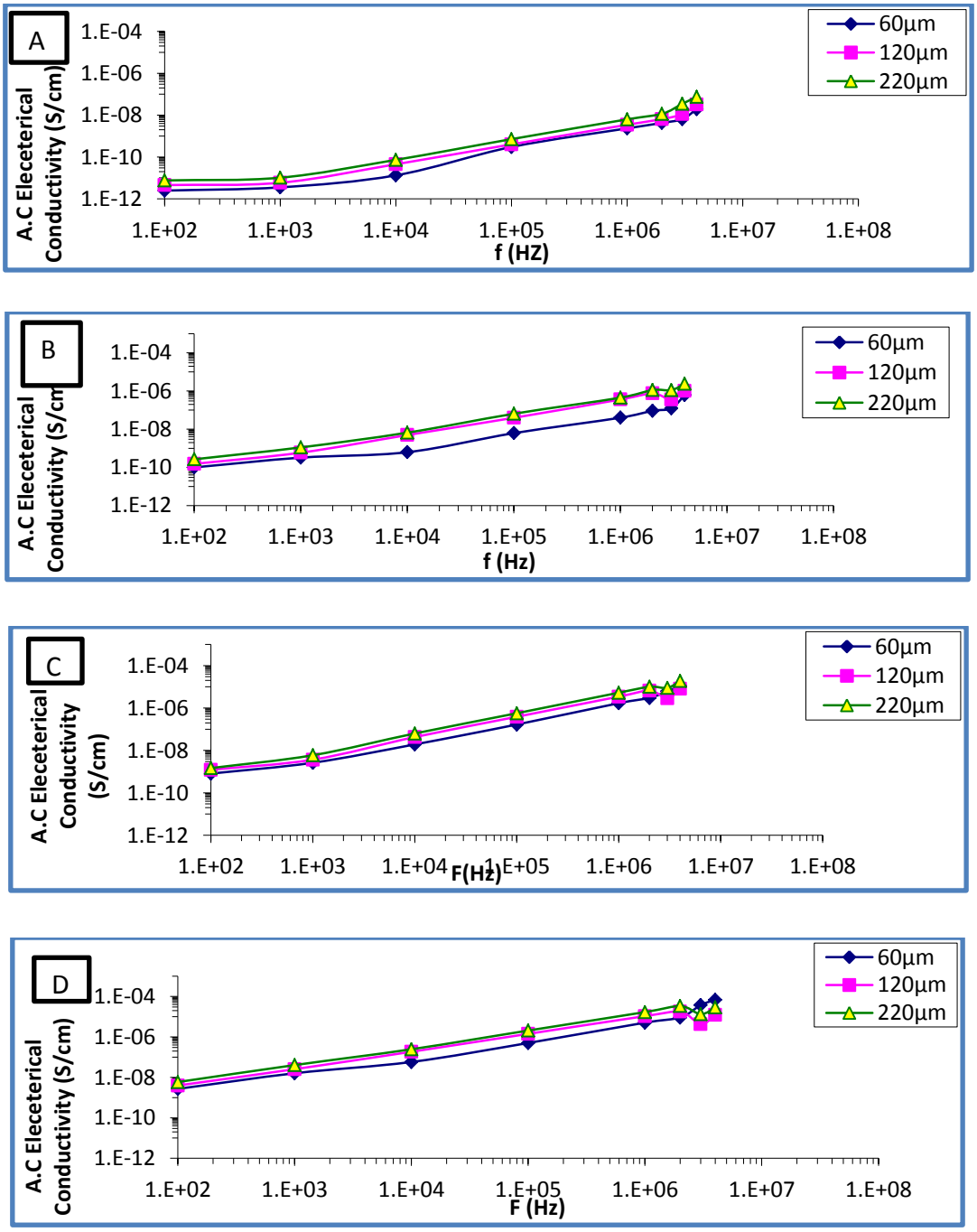

Fig(4.23): Electrical conductivity (s/cm) variation with frequency (Hz) for (PMMA-PbO) nanocomposites.

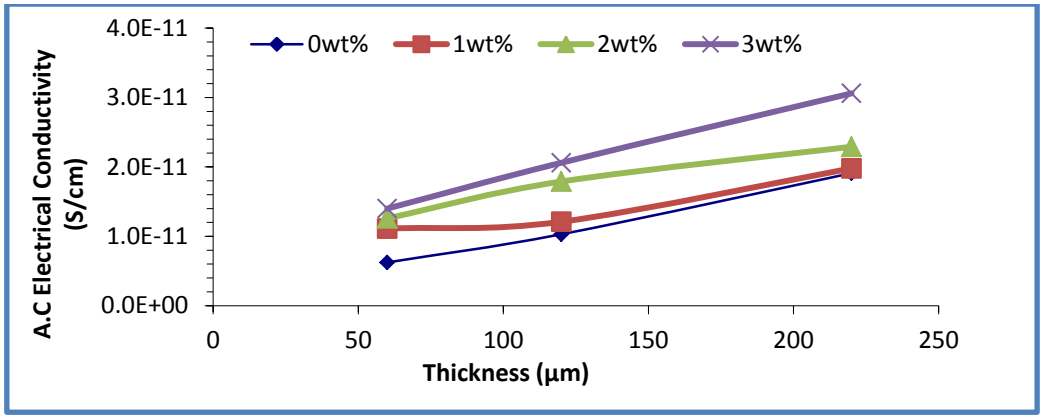

Figure (4.24): Variation in the alternating current conductivity (s/cm) of (PMMA-PbO) nanocomposites with different thicknesses.

4.5 Application of (PMMA-PbO) Nanocomposites for Gamma Ray Shielding.

Figure (4.25) show the variation of (N/N_0) for PMMA with different concentrations of (PbO) nanoparticles, and different thickness films. The transmission radiation decreases with the increasing of the concentrations of PbO nanoparticles which is attributed to the increase of the attenuation radiation, also the transmission radiation decreases with the thickness of the increased film which is attributed to the small number of particles of rays that pass through the films [129,130]. The variation in gamma radiation attenuation coefficients for PMMA as a function of film thickness at different concentrations (PbO) nanoparticles. As seen in Figure (4.26), attenuation coefficients rise as nanoparticle concentrations increase owing to gamma radiation absorption by nanocomposite shielding materials [131]. Attenuation coefficients increase with increased thicknesses of films because increasing the thickness of the film raises its resistance to radiation and hence the attenuation of radiation within the film [132,133]. From the figure, it showed good results compared to the results achieved by polymer composite with concrete Cs-137 shielding (μ=0.144cm^{-1}), however, composite polymer has an advantage over

concrete because of its mobility, less electrical properties and the ability to avoid neutron emission [134].

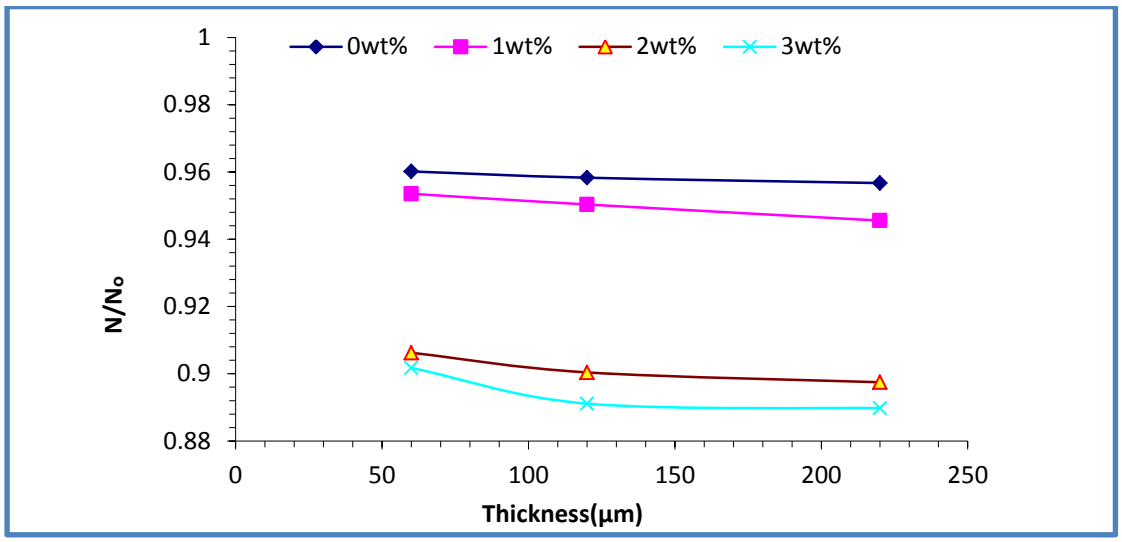

Figure (4.25): Variation of (N/N_o) for (PMMA-PbO) nanocomposites at different films thicknesses.

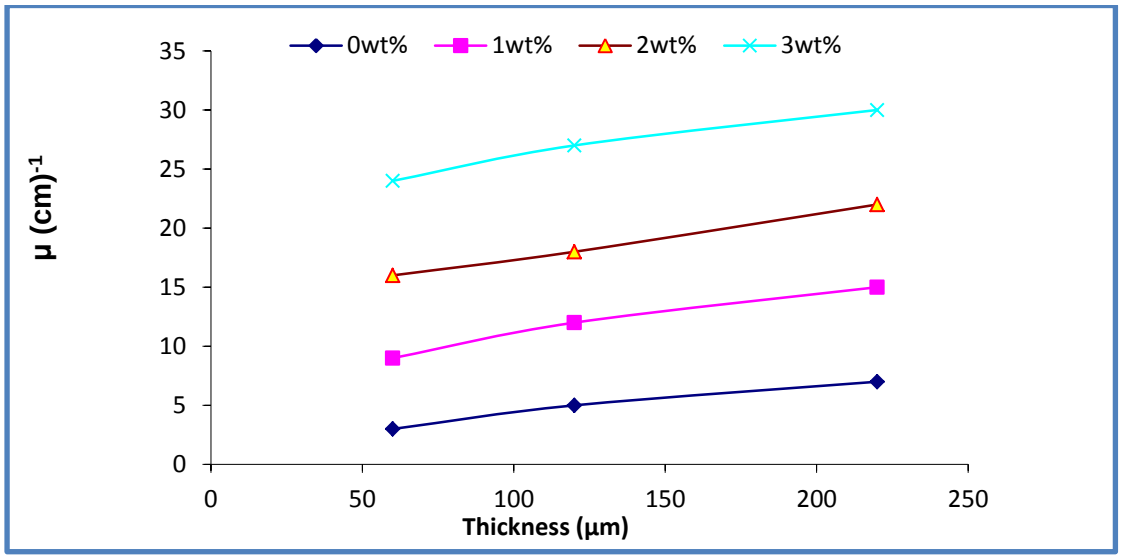

Figure (4.26): Variation of attenuation coefficients μ $(cm)^{-1}$ of gamma radiation for (PMMA-PbO) nanocomposites at different films thicknesses.

Chapter Five

Conclusions, and Future Works

5.1 Conclusions:

From the obtained results and discussions, the following points are concluded:

1- The optical microscope images show that Lead Oxide nanoparticles form a continuous network inside the polymer when the proportion of 3wt.%.

2- FT-IR spectra show shifts in some bands and changes in the intensities of other bands compared with pure PMMA films.

3- SEM shows the surface morphology of the (PMMA-PbO) nanocomposites films many aggregates or chunks randomly distributed on the top surface, homogeneous and coherent.

4- The extinction coefficient, refractive index, and dielectric constant (real, imaginary) increase as the thickness of the film and the concentrations of PbO nanoparticles rise. these properties can be used for films in coatings, microsensors, and the manufacture of food and drug preservation boxes.

5- The energy gap for indirect transition (allowed, forbidden) decreases with the increase of the film thickness and with the increasing concentrations of (PbO) nanoparticles.

6- As the frequency of the applied electric field increases, the dielectric constant and dielectric loss of the (PMMA-PbO) nanocomposites reduce, while electrical conductivity (A.C) of (PMMA-PbO) increases as the frequency is increased, these properties can be used for films in capacitors, transistor, and electronic circuits.

7- The dielectric constant, A.C electrical conductivity and the dielectric loss of (PMMA-PbO) nanocomposites for all

concentrations increase with increasing concentrations of lead oxide nanoparticles.

8- The maximum absorbance is in the UV region then this film can be used in attenuation of high-frequency radiation.

9- As the thickness of the film increases, the attenuation coefficients for gamma radiation increase.

5.2 Future Works :

1. Studying the mechanical and thermal properties of the (PMMA-PbO) nanocomposites.
2. Study of the pressure sensors application of the (PMMA-PbO) nanocomposites.
3. Effect of loading ratio of PbO nanoparticle on optical and electrical properties of (PMMA-PbO) nanocomposites.
4. Morphological and electrical properties of (PMMA-Ferrite material) nanocomposites and application.
5. Study of the humidity sensors application of the (PMMA-PbO) nanocomposites.
6. Study the effect of gamma rays on some physical properties of (PMMA- PbO) composite films.

References

References

[1] M. Subramanian, *Basics of polymers: fabrication and processing technology*. Momentum Press, 2015.

[2] D. Feldman, "Polymer history," *Des. Monomers Polym.*, vol. 11, no. 1, pp. 1–15, 2008.

[3] J. McMurry, "Organic chemistry," *Brooks/Cole, USA*, vol. 895, p. 1003, 2000.

[4] R. Oslanec, A. C. Costa, R. J. Composto, and P. Vlcek, "Effect of block copolymer adsorption on thin film dewetting kinetics," *Macromolecules*, vol. 33, no. 15, pp. 5505–5512, 2000.

[5] F. J. Davis, *Polymer chemistry: a practical approach*. Oxford University Press on Demand, 2004.

[6] D. I. Bower, "An introduction to polymer physics." American Association of Physics Teachers, 2003.

[7] M. Akay, *Introduction to polymer science and technology*. Bookboon, 2012.

[8] K. Gabur, "Preparation and study the electrical and optical properties of (PS-Ni) composites," *Unpubl. M. Sc. Thesis). Babylon Univ. Coll. Sci. Iraq*, 2010.

[9] G. Odian, "Principle of Polymerization, ; John &Son," *Inc New York*, 2004.

[10] A. Muheisin, "Study of electrical conductivity for amorphous and semi crystalline polymers filled with Lithium Fluoride Additive." M. Sc. Thesis, University of Mustansiriah, College of Science, 2009.

[11] A. I. Okele, "An Introduction to Polymers and Some Profiles of Polymer Industries in Nigeria," *SciFed J. Polym. Sci.*, 2017.

[12] C. Zweben and C. A. Harper, "Metal matrix composites, ceramic matrix composites, carbon matrix composites and thermally conductive polymers matrix composites," *Handb. Plast. Elastomers Compos.*, p. 35, 2002.

[13] R. M. Jones, "Mechanics of Composite Materials, p., 164-165." CRC Press, London, 1998.

References

[14] D. Hull and T. W. Clyne, "An Introduction to Composite Materials." Cambridge University Press, Cambridge, 1996.

[15] G. A. Kontos *et al.*, "Electrical relaxation dynamics in TiO_2-polymer matrix composites," *Express Polym Lett*, vol. 1, no. 12, pp. 781–789, 2007.

[16] J. Furer, "Growth of single-wall carbon nanotubes by chemical vapor deposition for electrical devices." University_of_Basel, 2006.

[17] J. Furer, "Electrochemically induced sol− gel preparation of single-crystalline TiO_2 nanowires," *Nano Lett.*, vol. 2, no. 7, pp. 717–720, 2002.

[18] P. G. Sheasby, R. Pinner, and S. Wernick, *The surface treatment and finishing of aluminium and its alloys*, vol. 1. ASM international Materials Park, OH, 2001.

[19] C. Buzea, I. I. Pacheco, and K. Robbie, "Nanomaterials and nanoparticles: sources and toxicity," *Biointerphases*, vol. 2, no. 4, pp. MR17–MR71, 2007.

[20] T. U. Eindhoven and D. Version, *Controlling the rheology of polymer / silica nanocomposites Controlling the rheology of polymer / silica nanocomposites*, no. 2010. 2020.

[21] A. H. Doulabi, K. Mequanint, and H. Mohammadi, "Blends and nanocomposite biomaterials for articular cartilage tissue engineering," *Materials (Basel).*, vol. 7, no. 7, pp. 5327–5355, 2014.

[22] G. A. P. Mariselvi, "Structural, Morphological and Antibacterial Activity of Kaolinite/TiO_2 Nanocomposites," *J. Nanosci. Technol.*, vol. 1, no. 1, pp. 16–18, 2015.

[23] T. A. Osswald, E. Baur, S. Brinkmann, K. Oberbach, and E. Schmachtenberg, "International plastics handbook," *Hanser, Munich*, p. 758, 2006.

[24] D. Dorranian, Z. Abedini, A. Hojabri, and M. Ghoranneviss, "Effects of Oxygen RF Plasma on Properties of Poly Methyl Methacrylate Polymer," *J. Theor. Appl. Phys. (IRANIAN Phys. JOURNAL)*, vol. 2, no. 1, pp. 17–21, 2008.

[25] D. Fischer, Y. Li, B. Ahlemeyer, J. Krieglstein, and T. Kissel, "In vitro

cytotoxicity testing of polycations: influence of polymer structure on cell viability and hemolysis," *Biomaterials*, vol. 24, no. 7, pp. 1121–1131, 2003.

[26] F. Fixe, M. Dufva, P. Telleman, and C. B. V. Christensen, "Functionalization of poly (methyl methacrylate)(PMMA) as a substrate for DNA microarrays," *Nucleic Acids Res.*, vol. 32, no. 1, pp. e9–e9, 2004.

[27] R. Çapan, A. K. Ray, A. K. Hassan, and T. Tanrisever, "Poly (methyl methacrylate) films for organic vapour sensing," *J. Phys. D. Appl. Phys.*, vol. 36, no. 9, p. 1115, 2003.

[28] F. W. Billmeyer, *Textbook of polymer science*. John Wiley & Sons, 1984.

[29] M. S. El-Bana, G. Mohammed, A. M. El Sayed, and S. El-Gamal, "P reparation and characterization of PbO/carboxymethyl cellulose/polyvinylpyrrolidone nanocomposite films," *Polym. Compos.*, vol. 39, no. 10, pp. 3712–3725, 2018.

[30] G. Xing *et al.*, "One-pot and high-yield preparation of ultrathin β-PbO nanowires and nanosheets for high-capacity positive electrodes in lead-acid batteries," *J. Alloys Compd.*, vol. 831, p. 154845, 2020.

[31] G. Hu *et al.*, "Electrosynthesis of Al/Pb/α-PbO_2 composite inert anode materials," *Trans. Nonferrous Met. Soc. China (English Ed.*, vol. 25, no. 6, pp. 2095–2102, 2015.

[32] T. L. Blair, "Lead oxide technology—past, present, and future," *J. Power Sources*, vol. 73, no. 1, pp. 47–55, 1998.

[33] P. P. Jeeju, S. Jayalekshmi, K. Chandrasekharan, and P. Sudheesh, "Enhanced linear and nonlinear optical properties of thermally stable ZnO/poly (styrene)–poly (methyl methacrylate) nanocomposite films," *Thin Solid Films*, vol. 531, pp. 378–384, 2013.

[34] K. Al-Ammar, A. Hashim, and M. Husaien, "Synthesis and study of optical properties of (PMMA-$CrCl_2$) composites," *Chem. Mater. Eng*, vol. 1, no. 3, pp. 85–87, 2013.

[35] W. A. Musa, T. K. Hamad, and M. T. A. Nabi, "Thickness Effect on the Optical Constants of Poly Methyl Methacrylate (PMMA) Doped by Potassium

Iodide," *Al-Nahrain J. Sci.*, vol. 16, no. 3, pp. 119–123, 2013.

[36] S. Sugumaran and C. S. Bellan, "Transparent nano composite PVA–TiO_2 and PMMA–TiO_2 thin films: Optical and dielectric properties," *Optik (Stuttg).*, vol. 125, no. 18, pp. 5128–5133, 2014.

[37] N. G. Hamed and M. Rahem, "To Study the Silver Concentration Effect on the Optical and Electrical Properties of the Ag/PMMA Composites," *Eng. Technol. J.*, vol. 32, no. 1 Part (B) Scientific, 2014.

[38] B. H. Rabee and B. A. Al-Kareem, "Study of optical properties of (PMMA-CuO) nanocomposites," *Int. J. Sci. Res. Vol.*, vol. 5, 2016.

[39] R. T. Abdulwahid, O. G. Abdullah, S. B. Aziz, S. A. Hussein, F. F. Muhammad, and M. Y. Yahya, "The study of structural and optical properties of PVA: PbO_2 based solid polymer nanocomposites," *J. Mater. Sci. Mater. Electron.*, vol. 27, no. 11, pp. 12112–12118, 2016.

[40] P. Maji, R. B. Choudhary, and M. Majhi, "Structural, optical and dielectric properties of ZrO_2 reinforced polymeric nanocomposite films of polymethylmethacrylate (PMMA)," *Optik (Stuttg).*, vol. 127, no. 11, pp. 4848–4853, 2016.

[41] J. K. Ahmed, R. M. A. Alradha, and N. I. Kareem, "Molecular interactions of poly (methyl methacrylate) and poly (vinyl alcohol) with chitosan polymer," *Acta Sci. Cancer Biol.*, vol. 3, no. 2, pp. 2–8, 2019.

[42] A. A. Abid, S. H. Al-nesrawy, and A. R. Abdulridha, "SYNTHESIS AND CHARACTERIZATION OF (PVA-PVP-CB) NANO COMPOSITES," *J. Crit. Rev.*, vol. 7, no. 15, pp. 2524–2532, 2020.

[43] A. A. Abid, S. H. Al-Nesrawy, and A. R. Abdulridha, "New Fabrication (PVA-PVP-C. B) Nanocomposites: Structural and Electrical Properties," *J. Phys. Conf. Ser.*, vol. 1804, no. 1, 2021.

[44] M. S. Toman and S. H. Al-nesrawy, "New Fabrication (PVA-CMC-PbO) Nanocomposites Structural and Electrical Properties," *NeuroQuantology*, vol. 19, no. 4, p. 38, 2021.

[45] M. A. Kadhim and E. Al-Bermany, "New fabricated PMMA-PVA/graphene oxide nanocomposites: Structure, optical properties and application," *J. Compos. Mater.*, vol. 55, no. 20, pp. 2793–2806, 2021.

[46] O. B. Fadil and A. Hashim, "Fabrication and Tailored Optical Characteristics of CeO_2/SiO_2 Nanostructures Doped PMMA for Electronics and Optics Fields," *Silicon*, pp. 1–8, 2022.

[47] J. F. Rabek, "Experimental methods in polymer chemistry," 1980.

[48] A. Telser, "Fundamentals of light microscopy and electronic imaging." LWW, 2002.

[49] A. Di Gianfrancesco, *Materials for ultra-supercritical and advanced ultra-supercritical power plants*. Woodhead Publishing, 2016.

[50] A. Ramírez-Hernández, C. Aguilar-Flores, and A. Aparicio-Saguilán, "Fingerprint analysis of FTIR spectra of polymers containing vinyl acetate," *Dyna*, vol. 86, no. 209, pp. 198–205, 2019.

[51] O. Faix, "Fourier transform infrared spectroscopy," in *Methods in lignin chemistry*, Springer, 1992, pp. 83–109.

[52] N. Jaggi and D. R. Vij, "Fourier transform infrared spectroscopy," in *Handbook of Applied Solid State Spectroscopy*, Springer, 2006, pp. 411–450.

[53] K. Latha, *Experiment and Evaluation in Information Retrieval Models*. Chapman and Hall/CRC, 2017.

[54] A. Khursheed, *Scanning electron microscope optics and spectrometers*. World scientific, 2011.

[55] O. P. Choudhary and P. Choudhary, "Scanning electron microscope: advantages and disadvantages in imaging components," *Int. J. Curr. Microbiol. Appl. Sci.*, vol. 6, no. 5, pp. 1877–1882, 2017.

[56] S. Naureen, "Top-down Fabrication Technologies for High Quality III-V Nanostructures." KTH Royal Institute of Technology, 2013.

[57] M. H. M. Zaid, K. A. Matori, S. H. Abdul Aziz, A. Zakaria, and M. S. M.

Ghazali, “Effect of ZnO on the physical properties and optical band gap of soda lime silicate glass,” *Int. J. Mol. Sci.*, vol. 13, no. 6, pp. 7550–7558, 2012.

[58] M. A. Habeeb, H. M. Mohssen, and R. G. Kadhim, “Effect of (CoO) Nanoparticles on Someoptical Properties of (PVA-Paam) Composite,” *Int. J. Eng. Res.*, vol. 3, no. 5, 2014.

[59] M. Sauer, J. Hofkens, and J. Enderlein, *Handbook of fluorescence spectroscopy and imaging: from ensemble to single molecules*. John Wiley & Sons, 2010.

[60] B. H. Rabee, F. Z. Razooqi, and M. H. Shinen, “Investigation of optical properties for (PVA-PEG-Ag) polymer nanocomposites films,” *Chem. Mater. Res.*, vol. 7, no. 4, pp. 103–109, 2015.

[61] A. D. A. Buba and J. S. A. Adelabu, “Optical and Electrical Properties of Chemically Deposited ZnO Thin Films,” *Pacific J. Sci. Technol.*, vol. 11, no. 2, pp. 429–434, 2010.

[62] D. A. Neamen, *Semiconductor physics and devices*. 1992.

[63] W. Klöpffer, “Infrared Spectroscopy of Polymers,” in *Introduction to Polymer Spectroscopy*, Springer, 1984, pp. 75–107.

[64] C. Mwolfe, N. Holouyak, and G. B. Stillman, “Physical properties of Semiconductor,” *Printice Hall, New York*, 1989.

[65] L. Qian and J. P. Hinestroza, “Application of nanotechnology for high performance textiles,” *J. Text. apparel, Technol. Manag.*, vol. 4, no. 1, pp. 1–7, 2004.

[66] G. Attia and M. F. H. Abd El-kader, “Structural, optical and thermal characterization of PVA/2HEC polyblend films,” *Int. J. Electrochem. Sci*, vol. 8, no. 4, pp. 5672–5687, 2013.

[67] S. L. Chuang, “Optical Processes in Semiconductors,” *Phys. Photonic Devices, 2nd ed.; Boreman, G., Ed*, pp. 347–389, 2009.

[68] A. M. Andriesh, M. S. Iovu, and S. D. Shutov, “Chalcogenide non-crystalline semiconductors in optoelectronics,” *J. Optoelectron. Adv. Mater*, vol. 4, no. 3,

pp. 631–647, 2002.

[69] C. Kittel, “Introduction to solid state physics,” 1976.

[70] J. I. Pankove, *Optical processes in semiconductors*. Courier Corporation, 1975.

[71] A. Naser M, S. Zaliman, H. Uda, and A.-D. Yarub, “Investigation of the absorption coefficient, refractive index, energy band gap, and film thickness for Al0. 11Ga0. 89N, Al0. 03Ga0. 97N, and GaN by optical transmission method,” 2009.

[72] D. L. Makhija, K. D. Patel, V. M. Pathak, and R. Srivastava, “Optical transitions in WSe_2 single crystals,” *J. Ovonic Res. Vol*, vol. 4, no. 6, pp. 141–145, 2008.

[73] J. I. Pankove, “Optical processes on semiconductors Dover publication,” *Inc. New york*, 1971.

[74] R. G. Kadhim, “Study of some optical properties of polystyrene-Copper nanocomposite films,” *World Sci. News*, vol. 30, pp. 14–25, 2016.

[75] J. H. Nahida, “Spectrophotometric analysis for the UV-irradiated (PMMA),” *Int. J. Basic Appl. Sci.*, vol. 12, no. 2, pp. 58–67, 2012.

[76] A. H. Ahmad and A. M. Awatif, “Dopping effect on optical constants of polymethylmethacrylate (PMMA),” *Eng. Technol. J.*, vol. 25, no. 4, 2007.

[77] R. A. Berglund, P. B. Graham, and R. S. Miller, “Applications of in-situ FT-IR in Pharmaceutical Process R&D,” *Spectrosc. THEN EUGENE-*, vol. 8, p. 31, 1993.

[78] A. H. Ahmed, “Doping effect on optical constant of polymethylmethacrlate,” *Eng. Technol.*, vol. 25, no. 4, 2007.

[79] S. M. Sze and K. K. Ng, “Physics of Semiconductor Devices, John Wiley & Sons,” *New York*, vol. 68, 1981.

[80] D. M. Bigg, “Mechanical, thermal, and electrical properties of metal fiber-filled polymer composites,” *Polym. Eng. Sci.*, vol. 19, no. 16, pp. 1188–1192, 1979.

References

[81] N. Saba, P. M. Tahir, and M. Jawaid, "A review on potentiality of nano filler/natural fiber filled polymer hybrid composites," *Polymers (Basel).*, vol. 6, no. 8, pp. 2247–2273, 2014.

[82] H.-G. Elias, "Polynucleotides," in *Macromolecules*, Springer, 1977, pp. 1025–1036.

[83] N. K. Abbas, M. A. Habeeb, and A. J. K. Algidsawi, "Preparation of chloro penta amine cobalt (III) chloride and study of its influence on the structural and some optical properties of polyvinyl acetate," *Int. J. Polym. Sci.*, vol. 2015, 2015.

[84] H. I. Jafar, N. A. Ali, and A. Shawky, "Study of AC electrical properties of aluminum–epoxy composites," *Al-Nahrain J. Sci.*, vol. 14, no. 3, pp. 77–82, 2011.

[85] T. Seghier and F. Benabed, "Dielectric proprieties determination of high density polyethylene (HDPE) by dielectric spectroscopy," *Int. J. Mater. Mech. Manuf.*, vol. 3, no. 2, 2015.

[86] S. Shekhar, V. Prasad, and S. V Subramanyam, "Structural and electrical properties of composites of polymer–iron carbide nanoparticles embedded in carbon," *Mater. Sci. Eng. B*, vol. 133, no. 1–3, pp. 108–112, 2006.

[87] C. C. Ku and R. Liepins, *Electrical properties of polymers*. Hanser publishers Munich, 1987.

[88] A. R. Blythe, T. Blythe, and D. Bloor, *Electrical properties of polymers*. Cambridge university press, 2005.

[89] J. Hladik, *Physics of electrolytes*, vol. 1. Academic Press, 1972.

[90] N. A. Azahari, N. Othman, and H. Ismail, "Biodegradation studies of polyvinyl alcohol/corn starch blend films in solid and solution media," *J. Phys. Sci.*, vol. 22, no. 2, pp. 15–31, 2011.

[91] R. I. Khaleel, "Electrical and Optical properties modification of Poly (Vinyl Chloride) by Zinc, Copper and Nickel Ethyl Xanthate chelate Complexes," *M. Sc., Coll. Sci., Mustansiryah*, vol. 1, pp. 21–41, 2004.

References

[92] R. Tomar and C. R. Sharma, "Studies on conducting PVP polymer composites for AC conduction," *Int. J. Sci. Engg. Technol. Res*, vol. 3, pp. 3023–3026, 2014.

[93] I. Yücedağ, A. Kaya, Ş. Altındal, and I. Uslu, "Frequency and voltage-dependent electrical and dielectric properties of Al/Co-doped PVA/p-Si structures at room temperature," *Chinese Phys. B*, vol. 23, no. 4, p. 47304, 2014.

[94] I. Teraoka, "Polymer solutions: an introduction to physical properties," 2002.

[95] S. Zhang, Q. Tao, Z. Wang, and Z. Zhang, "Controlled heat release of new thermal storage materials: the case of polyethylene glycol intercalated into graphene oxide paper," *J. Mater. Chem.*, vol. 22, no. 38, pp. 20166–20169, 2012.

[96] G. K. R. AL-Morshdy, "Effect of addition ferrous chloride ($FeCl_2$) on some AC and DC electrical properties of polystyrene," *J. Babylon Univ. Appl. Sci.*, no. 7, 2013.

[97] N. Mohd Noor, "Investigate the Dispersion and Suspension of Zinc and Silver Nano additives in Nano composites," 2013.

[98] R. M. Paroli, K. K. Y. Liu, and T. R. Simmons, *Thermoplastic polyolefin roofing membranes*. Citeseer, 1999.

[99] M. K. Roy, R. G. Mahloniya, J. Bajpai, and A. K. Bajpai, "Spectroscopic and morphological evaluation of gamma radiation irradiated polypyrole based nanocomposites," *J Adv Mater Lett*, vol. 3, no. 5, pp. 426–432, 2012.

[100] G. A. Eid, A. I. Kany, M. M. El-Toony, I. I. Bashter, and F. A. Gaber, "Application of epoxy/Pb_3O_4 composite for gamma ray shielding," *Arab. J. Nucl. Sci. Appl*, vol. 46, no. 2, pp. 226–233, 2013.

[101] K. J. Singh, N. Singh, R. S. Kaundal, and K. Singh, "Gamma-ray shielding and structural properties of PbO–SiO_2 glasses," *Nucl. Instruments Methods Phys. Res. Sect. B Beam Interact. with Mater. Atoms*, vol. 266, no. 6, pp. 944–948, 2008.

References

[102] J. Ramesh Babu and K. Vijaya Kumar, "Studies on structural and electrical properties of $NaHCO_3$ doped PVA films for electrochemical cell applications," *Chemtech*, vol. 7, pp. 1–171, 2014.

[103] J. P. Sharma and S. S. Sekhon, "Nanodispersed polymer gel electrolytes: Conductivity modification with the addition of PMMA and fumed silica," *Solid State Ionics*, vol. 178, no. 5–6, pp. 439–445, 2007.

[104] R. L. Sakaguchi and J. M. Powers, *Craig's restorative dental materials-e-book*. Elsevier Health Sciences, 2012.

[105] S. El-Gamal and M. Elsayed, "Synthesis, structural, thermal, mechanical, and nano-scale free volume properties of novel PbO/PVC/PMMA nanocomposites," *Polymer (Guildf).*, vol. 206, p. 122911, 2020.

[106] V. N. Suryawanshi, A. S. Varpe, and M. D. Deshpande, "Band gap engineering in PbO nanostructured thin films by Mn doping," *Thin Solid Films*, vol. 645, pp. 87–92, 2018.

[107] M. L. Hernández, L. M. Alonso, M. M. Pradas, O. E. L. Lozano, and D. G. Bello, "Composites of poly (methyl methacrylate) with hybrid fillers (micro/nanohydroxyapatite): Mechanical, setting properties, bioactivity and cytotoxicity in vitro," *Polym. Compos.*, vol. 34, no. 11, pp. 1927–1937, 2013.

[108] S. M. Sze, Y. Li, and K. K. Ng, *Physics of semiconductor devices*. John wiley & sons, 2021.

[109] J. I. Kroschwitz, *Electrical and electronic properties of polymers: A state-of-the-art compendium*. Wiley-Interscience, 1988.

[110] E. Rouaramadan and A. A. Hasan, "Study of the optical constants of the PVC/PMMA blends," *Int. J. Appl. or Innov. Eng. Manag.*, vol. 2, no. 11, pp. 240–243, 2013.

[111] H. Hakim, A. Hashim, S. Sabah, and N. Mohammad, "Preparation of (PMMA-Y_2O_3) Nanocomposites and Study their Optical Properties," *J. Ind. Eng. Res.*, vol. 1, p. 3, 2015.

[112] M. Fox, "Optical properties of solids." American Association of Physics

Teachers, 2002.

[113] E. Tang, G. Cheng, and X. Ma, "Preparation of nano-ZnO/PMMA composite particles via grafting of the copolymer onto the surface of zinc oxide nanoparticles," *Powder Technol.*, vol. 161, no. 3, pp. 209–214, 2006.

[114] A. Hashim, "Enhanced structural, optical, and electronic properties of In_2O_3 and Cr_2O_3 nanoparticles doped polymer blend for flexible electronics and potential applications," *J. Inorg. Organomet. Polym. Mater.*, vol. 30, no. 10, pp. 3894–3906, 2020.

[115] F. S. Ahmed, N. Y. Ahmed, R. S. Ali, N. F. Habubi, K. H. Abass, and S. S. Chiad, "Effects of substrate type on some optical and dispersion properties of sprayed CdO thin films," *NeuroQuantology*, vol. 18, no. 3, p. 56, 2020.

[116] K. H. Abass, A. Adil, and M. K. Mohammed, "Fabrication and Enhancement of SnS: Ag/Si Solar Cell Via Thermal Evaporation Technique," *J. Eng. Appl. Sci.*, vol. 13, no. 4, pp. 919–925, 2018.

[117] M. R. Islam and J. Podder, "Optical properties of ZnO nano fiber thin films grown by spray pyrolysis of zinc acetate precursor," *Cryst. Res. Technol. J. Exp. Ind. Crystallogr.*, vol. 44, no. 3, pp. 286–292, 2009.

[118] Z. S. Obaid, "Physical Properties of PMMA/ZnO Composite Material." Ministry of Higher Education, 2017.

[119] B. K. H. Al-Maiyaly, "The Effect of Thickness on Electrical Conductivity and Optical Constant of Fe_2O_3 Thin Films," *Ibn AL-Haitham J. Pure Appl. Sci.*, vol. 27, no. 3, pp. 237–246, 2017.

[120] G. Patel, M. B. Sureshkumar, and P. Patel, "Effect of TiO_2 on optical properties of PMMA: an optical characterization," in *Advanced Materials Research*, 2012, vol. 383, pp. 3249–3256.

[121] Ü. Alver *et al.*, "Optical and dielectric properties of PMMA/α-Fe_2O_3–ZnO nanocomposite films," *J. Inorg. Organomet. Polym. Mater.*, vol. 29, no. 5, pp. 1514–1522, 2019.

[122] M. Haneef, H. Saleem, and A. Habib, "Use of graphene nanosheets and barium

titanate as fillers in PMMA for dielectric applications," *Synth. Met.*, vol. 223, pp. 101–106, 2017.

[123] S. Devikala, P. Kamaraj, and M. Arthanareeswari, "AC conductivity studies of PMMA/TiO_2 composites," *Mater. Today Proc.*, vol. 5, no. 2, pp. 8678–8682, 2018.

[124] S. A. Salman, Z. A. Al-Ramadhan, and Z. F. Nazal, "Optical properties of polyvinyl alcohol (PVA) films doped with $CoCH_3COOH$ salt.," *alcohol*, vol. 2, p. 3, 2014.

[125] S. Satapathy, P. K. Gupta, K. B. R. Varma, P. Tiwari, and V. Ganeshan, "Study on dielectric behavior of Lithium Tantalate (LT) nano particle filled poly (vinylidene fluoride)(PVDF) nano composite," *arXiv Prepr. arXiv0808.0420*, 2008.

[126] B. Abd-Alkareem, "Effect of Nano-Copper Oxide on the Electrical and Optical Properties of (PMMA) Polymer." College of Education for pure sciences, University of Babylon, 2016.

[127] K. Rajesh, V. Crasta, N. B. Rithin Kumar, G. Shetty, and P. D. Rekha, "Structural, optical, mechanical and dielectric properties of titanium dioxide doped PVA/PVP nanocomposite," *J. Polym. Res.*, vol. 26, no. 4, pp. 1–10, 2019.

[128] F. Gmati, A. Fattoum, N. Bohli, and A. B. Mohamed, "Effects of the molar mass of the matrix on electrical properties, structure and morphology of plasticized PANI–PMMA blends," *J. Phys. Condens. Matter*, vol. 20, no. 12, p. 125221, 2008.

[129] T. Bel, C. Arslan, and N. Baydogan, "Radiation shielding properties of poly (methyl methacrylate)/colemanite composite for the use in mixed irradiation fields of neutrons and gamma rays," *Mater. Chem. Phys.*, vol. 221, pp. 58–67, 2019.

[130] B. E. Yoldas, "Investigations of porous oxides as an antireflective coating for glass surfaces," *Appl. Opt.*, vol. 19, no. 9, pp. 1425–1429, 1980.

References

[131] A. J. Kadham, D. Hassan, N. Mohammad, and A. Hashim, “Fabrication of (polymer blend-magnesium oxide) nanoparticle and studying their optical properties for optoelectronic applications,” *Bull. Electr. Eng. Informatics*, vol. 7, no. 1, pp. 28–34, 2018..

[132] R. Rohini and S. Bose, “Electromagnetic interference shielding materials derived from gelation of multiwall carbon nanotubes in polystyrene/poly (methyl methacrylate) blends,” *ACS Appl. Mater. Interfaces*, vol. 6, no. 14, pp. 11302–11310, 2014.

[133] M. A. Kiani, S. J. Ahmadi, M. Outokesh, R. Adeli, and H. Kiani, “Study on physico-mechanical and gamma-ray shielding characteristics of new ternary nanocomposites,” *Appl. Radiat. Isot.*, vol. 143, pp. 141–148, 2019.

[134] I. Akkurt, H. Akyildirim, B. Mavi, S. Kilincarslan, and C. Basyigit, “Gamma-ray shielding properties of concrete including barite at different energies,” *Prog. Nucl. Energy*, vol. 52, no. 7, pp. 620–623, 2010.

الخلاصة

توصلت هذه الدراسة إلى تأثير سمك الغشاء على الخواص الكهربائية والبصرية للمتراكبات النانوية (PMMA-PbO). تم تحضير المتراكبات النانوية (PMMA-PbO) بطريقة الصب ، بمتوسط حجم جزيئي 66 نانومتر ونسب وزن من جزيئات أوكسيد الرصاص النانوية (0, 1, 2, 3)wt% ، تم استخدام ميكرومتر لتحديد سمك العينات ، ووجد أنها في حدود (60,120,220)µm.

أظهرت صور المجهر الضوئي أن جزيئات أوكسيد الرصاص النانوية تشكل شبكة مستمرة داخل البوليمر عند 3wt.%. تظهر أطياف FTIR إزاحه في بعض النطاقات وتغير في الشدة ، وهذا يشير إلى عدم وجود تفاعل كيميائي ، بل يشير إلى حدوث الترابط الفيزيائي. وقد تم الكشف عن التشكيل السطحي لأغشية المتراكبات النانوية (PMMA-PbO) عن طريق المجهر الإلكتروني الماسح (SEM) ، والذي يكشف عن العديد من المجاميع الموزعة عشوائياً على السطح العلوي ، والتي تكون متجانسة ومتماسكة.

أظهرت الخواص البصرية أن الامتصاصية ومعامل الامتصاص ومعامل الخمود ومعامل الانكسار وثابت العزل (الحقيقي ، والخيالي) تزداد مع زيادة سمك الأغشية وتراكيز الجسيمات النانوية (PbO). تقل فجوة الطاقة مع زيادة سمك الغشاء وتركيز الجسيمات النانوية لأوكسيد الرصاص.

يتزايد ثابت العزل وفقد العازل والتوصيل الكهربائي للمتراكبات النانوية (PMMA-PbO) مع زيادة سمك الأغشية وتركيز الجسيمات النانوية PbO. بينما يناقص ثابت العزل الكهربائي ، وفقدان العزل الكهربائي للمتراكبات النانوية (PMMA-PbO) مع زيادة شدة المجال الكهربائي المسلط ، من ناحية أخرى ، تزداد الموصلية الكهربائية AC مع زيادة التردد.

بما أن هذه المتراكبات النانوية تمتص بصورة جيدة عند الترددات العالية فأنها تستخدم في توهين الأشعاعات مثل أشعة جاما. تظهرالمتراكبات النانوية (PMMA-PbO) معاملات توهين خطية جيدة لإشعاع أشعة جاما

جمهورية العراق
وزارة التعليم العلي والبحث العلمي
جامعة بابل
كلية التربية للعلوم الصرفة
قسم الفيزياء

تأثير السمك على الخواص البصرية و الكهربائية للمتراكب النانوي (بولي مثيل ميثا اكريليت – أوكسيد الرصاص) وتطبيقاتها

رسالة مقدمة
إلى مجلس كلية التربية للعلوم الصرفة في جامعة بابل كجزء من متطلبات
نيل درجة الماجستير في التربية / الفيزياء

من قبل

بشائر عايد كاظم مطرود

بكالوريوس تربية فيزياء

جامعة كربلاء 2019م

بأشراف

أ.د.سمير حسن هادي النصراوي

1444 هـ 2022م